THE
ASTROPHYSICAL JOURNAL
AN INTERNATIONAL REVIEW OF SPECTROSCOPY
AND ASTRONOMICAL PHYSICS

VOLUME XXXVI NOVEMBER 1912 NUMBER 4

THE ATTRACTION OF SUN-SPOTS FOR PROMINENCES

By FREDERICK SLOCUM

In the autumn of 1910 a large group of sun-spots passed several times across the face of the sun. Its first passage was from August 2 to August 15. It was then given the Greenwich number 6874. The group consisted of a large regular spot, crossed by bright bridges, and accompanied by several small spots. It reappeared on August 31, as Greenwich No. 6880, and passed around the west limb on September 11. On the third apparition, from September 27 to October 8, the group was greatly extended. The main spot with its immediate attendants was numbered 6894, and a stream of spots just preceding 6893. The whole disturbed area was covered with calcium flocculi extending from latitude $-10°$ to latitude $-25°$, and from longitude 32° to longitude 65°. Its appearance on October 1, as photographed in the light of calcium with the spectroheliograph, is shown on Plate XII.

This same region returned to view on October 22, but the big spot had vanished and only a large area of bright flocculi remained to mark the place. Throughout its history this group was the scene of great activity. Bright eruptions were constantly appearing and disappearing, and, on several dates, dark flocculi were observed in the immediate vicinity. Photographs of the H and K region of the spectrum of various parts of the spot-group show

distortions and displacements, corresponding to velocities up to 40 km per second.

The particular features, however, to which I wish to call attention, are the forms and movements of the prominences which were associated with this disturbed area. Active prominences were observed in this region from August 2 to November 5, but the best displays occurred on the west limb on October 8 and on the east limb on October 22. On the former date nine photographs were secured, of which six are reproduced in Plate XI.

The spot-group at this time was very near the limb, as shown in Figs. 1 and 2, Plate XII. Fig. 1 is a low-level view and Fig. 2, high-level, both taken in the light of calcium. On account of the foreshortening, comparatively little idea of the great extent of the group can be derived from pictures taken so near the limb. I have, therefore, shown in Figs. 3 and 4, Plate XII, the high- and low-level appearance of the region when it was near the central meridian of the sun's disc. On Plate XI the position of the center of the largest spot of the group is indicated by the tip of the arrow.

The most striking feature of the views on this plate is that the prominences are pouring from both sides apparently right down into the big spot. There can be no question about the direction of motion, for a sufficient number of details can be identified on two or more plates to establish this. For example, note the three bright knots on the long streamer coming in from the right at $4^{h}26^{m}.6$ and $4^{h}34^{m}.9$, Plate XI. These three knots give velocities along the apparent trajectory of 16, 20, and 60 km per second, at distances of 170,000, 130,000, and 75,000 km from the center of attraction. The values of the velocities as well as the distances are, of course, affected by an unknown component in the line of sight, but, since these three points are upon the same trajectory, an accelerated velocity is undoubtedly indicated. Other points that can be identified on two plates give apparent velocities ranging from 15 to 90 km per second.

In addition to the general attraction manifested by this spot, there are also evidences of repulsion. The plates taken at $3^{h}24^{m}.9$ and $5^{h}26^{m}.5$ show bright straight jets coming directly out of the spot. These are generally so short-lived that they do not appear

PLATE XI

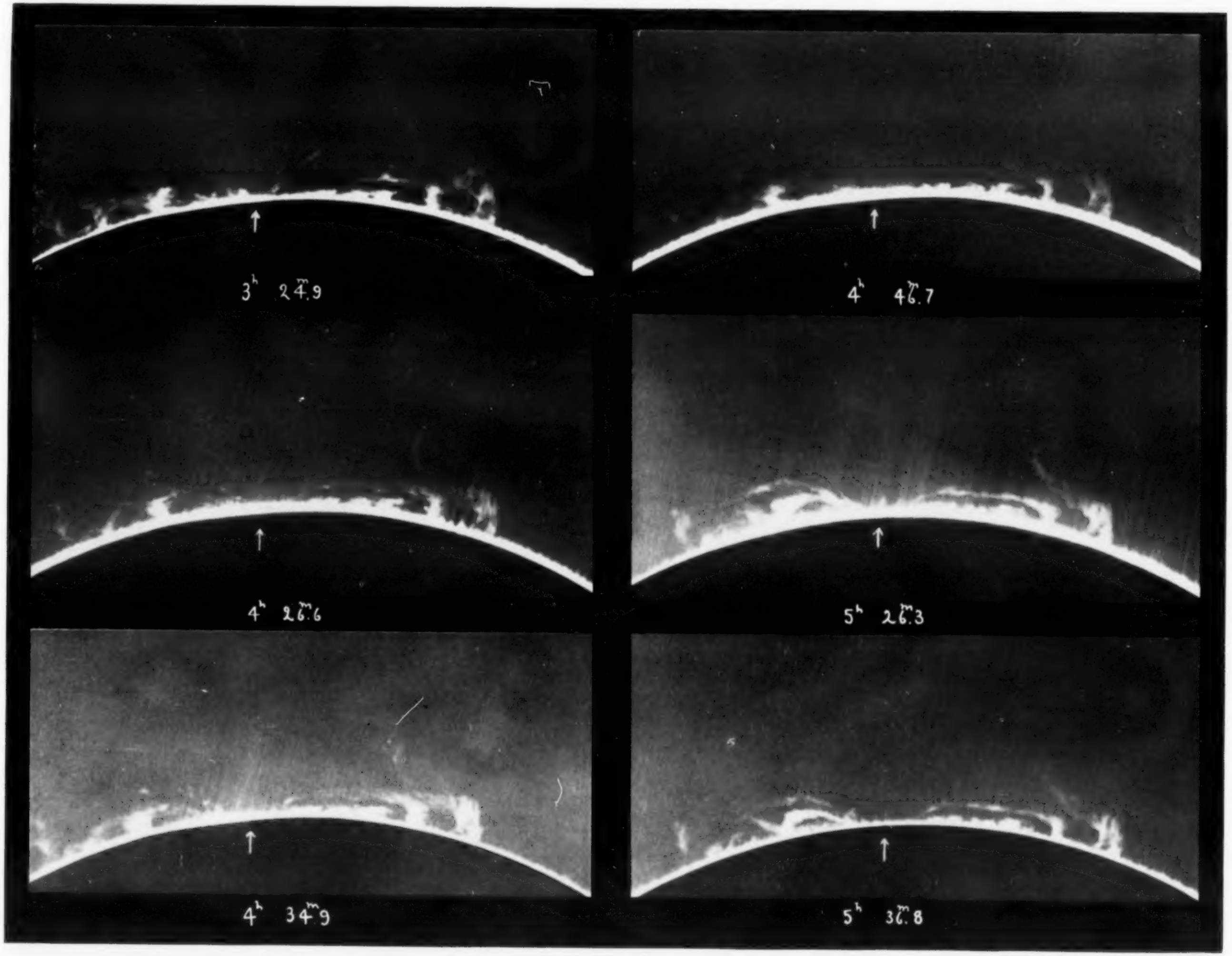

Calcium Spectroheliograms of Solar Prominences on October 8, 1910

Scale: 1 mm = 8600 km

PLATE XII

N

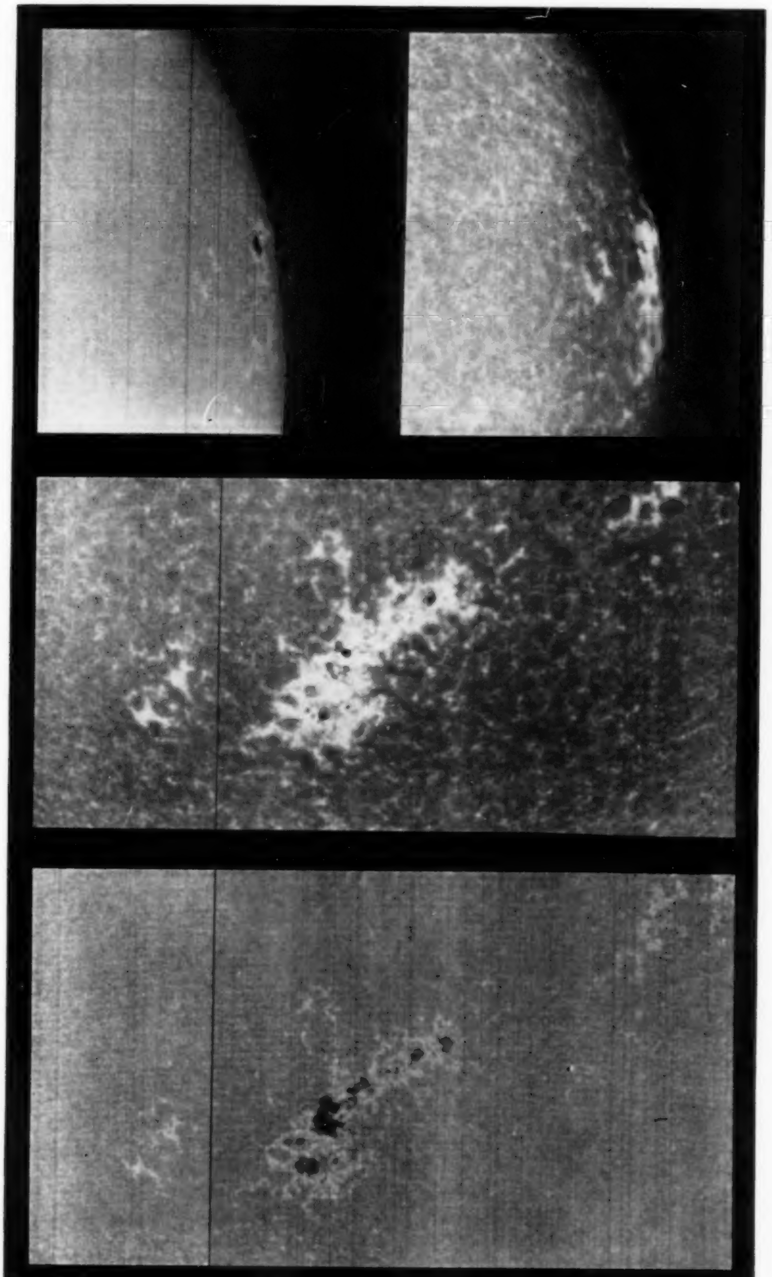

Fig. 1

Oct. 8
5h 41m
H₁

Fig. 2

Oct. 8
6h 17m
G.M.T.
H₂

E

Fig. 3

Oct. 1
4h 5m
H₂

Fig. 4

Oct. 1
4h 7m
H₁

SPECTROHELIOGRAMS OF SUN-SPOTS, OCTOBER 1 AND 8, 1910
Scale: 1 mm = 7900 km

PLATE XIII

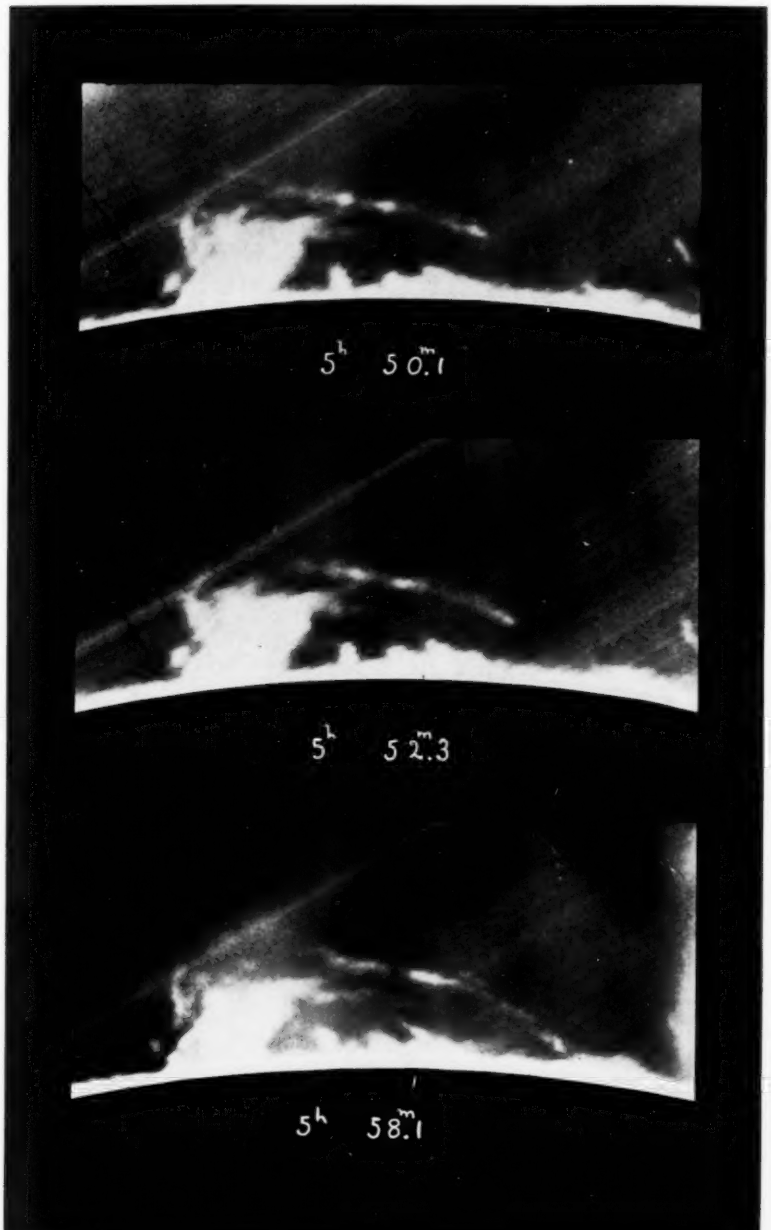

Calcium Spectroheliograms of Solar Prominences on October 22, 1910
Scale: 1 mm = 3500 km

on consecutive plates. One such eruption, however, can be identified on plates taken at $5^h43^m.7$ and $5^h50^m.5$, and this shows a velocity of ascent of 40 km per second, at a distance of 60,000 km from the spot.

A remarkable feature shown by this group of prominences is the great distance to which the influence of the spot is exerted. The prominences covered 45° of the sun's limb, with the spot nearly in the center, and the prominence matter, as far as 260,000 km from the spot, is evidently drawn in toward it. This is especially well shown to the right, or south, of the spot, where two centers of activity will be noticed. From the one nearer the spot, a stream of matter travels a long distance parallel to the surface of the sun and then bends down into the spot. From the prominence on the extreme right, a similar stream of matter starts off in the same direction, but, as it rises a trifle above the former stream, it apparently meets a counter current and is turned back, curving up to a height of $2\frac{1}{2}'$, or 107,000 km. This is best shown at $4^h34^m.9$.

This group of prominences of October 8 extended from latitude +6° to latitude −37° on the west limb. When this same region came to the east limb on October 22, a similar display of prominence activity was observed, extending from latitude +12° to latitude −36°. The sun-spot was no longer visible, but the prominences were gathered around the extensive area of bright flocculi, which still marked the place. To the north of the flocculi were numerous jets and prominences of frail structure, one of which rose to a height of $3\frac{1}{2}'$ or 150,000 km. To the south was a very bright and massive prominence, from the top of which poured a stream of matter down into the southern edge of the flocculi, striking the surface of the sun a few degrees south of where the big spot had been two weeks before.

I was fortunate enough to catch this stream in the act of descending. See Plate XIII. Between $5^h50^m.1$ and $5^h52^m.3$ the apparent velocity of the point of the stream was 87 km per second, and between $5^h52^m.3$ and $5^h58^m.1$, 110 km per second, again indicating acceleration. The small detached mass on the extreme right of the pictures of Plate XIII was descending at the rate of 10,000 km per second.

The above observations show that sun-spots, or the regions of sun-spot activity, exert a strong attraction upon some prominences.

In 1908, Professor Hale[1] reported a somewhat similar observation upon a dark hydrogen flocculus in the vicinity of a sun-spot. The flocculus approached the spot at velocities ranging from 140 to 76 km per second.

Again Evershed,[2] in his spectroscopic study of the radial motions around sun-spots, finds that "the gases of the higher chromosphere, hydrogen and calcium, show a tendency to move inward with a diminishing velocity toward the spot center."

In one respect the results of my observations differ from both those of Hale and of Evershed. My results show an acceleration toward the center, while theirs indicate diminishing velocities.

YERKES OBSERVATORY
August 10, 1912

[1] *Astrophysical Journal*, **28**, 109, 1908.

[2] *Memoirs of the Kodaikanal Observatory*, Vol. 1, Part 1, p. 54, 1909.

ELEMENTS OF THE ECLIPSING VARIABLES *W DELPHINI, S CANCRI, SW CYGNI, AND U CEPHEI*

By HARLOW SHAPLEY

For the reasons given in the preceding paper,[1] the most satisfactory eclipsing stars for the detection of darkening at the limb from the light-curve of the principal minimum, and most suitable for the critical application of the above methods, are those whose curves are thoroughly determined by the photometric work of an experienced observer, and which show a constant phase at minimum of sufficient length with respect to the depth to insure that the eclipse is total rather than annular. Among the best existing photometric observations of variables are those made with a polarizing photometer at the Harvard Observatory by Professor Wendell, and the four stars, *W Delphini*, *S Cancri*, *SW Cygni*, and *U Cephei*, for which he publishes observations in *Harvard Annals*, 69, Part I, satisfy the requirements.[2] No other total eclipses have been sufficiently well observed to be included; and, moreover, it would be a doubtful advantage for the present study to introduce work by another observer and another instrument into this homogeneous set of data. The following table of information concerning the four selected stars is taken from Wendell's summary.[3]

Star	R.A. 1900			Dec. 1900	Max.	Min.	Period	No. Obs.	Av. Dev.
	h	m	s		mg	mg			mg
W Delphini . .	20	33	7	$+17°55'.9$	9.39	12.11	$4^{d}.8061$	500	0.053
S Cancri	8	38	14	+19 23.6	8.00	10.10	9.4845485	407	0.040
S W Cygni . . .	20	3	50	+46 0.5	9.06	11.72	4.57294	192	0.029
U Cephei	0	53	24	+81 20.3	6.82	9.18	2.4928840	695*	0.055

* Erroneously 691 in Wendell's summary.

[1] *Astrophysical Journal*, **36**, 239, 1912.

[2] It is hardly necessary to show the impossibility of annular eclipses for these stars. The light lost at primary minimum is $2^{mg}.7$, $2^{mg}.1$, $2^{mg}.7$, and $2^{mg}.4$, respectively. Therefore, for annular eclipses by a totally obscure companion, the k's must necessarily be greater than 0.95, 0.92, 0.95, and 0.94, and must be still nearer unity if the companions are not wholly dark. The duration of constant minimum light in each case, as well as the general shape of the light-curve, immediately excludes such large values of k.

[3] *Harvard Annals*, **69**, 96.

The values of maximum and minimum light differ slightly from those used below which were determined by a more detailed consideration of the observations. The last column contains Wendell's determination of the average deviation of a single observation from the mean light-curve. The observations were made throughout the interval from October 1895 to December 1902. They represent a total of 28,704 comparisons of the light of the variables with that of their reference stars. All four stars belong to spectral class A.

1. *W Delphini*.—The 500 observations of this star have been discussed, and "uniform" elements derived, by Professor Russell, who publishes the orbit in the September number of this *Journal* as a part of his third paper on eclipsing variables. The table of normal places is reproduced here with an additional column of residuals.

NORMAL MAGNITUDES OF *W Delphini*

Phase	Mag.	No. Obs.	O.−C.$_u$	O.−C.$_d$	Phase	Mag.	No. Obs.	O.−C.$_u$	O.−C.$_d$
	mg		mg	mg		mg		mg	mg
−0^{d}2894..	9.41	6	+0.01	−0.01	+0^{d}0560..	11.76	7	−0.01	0.00
.2637..	9.49	5	+ .02	.00	.0659..	11.58	8	+ .01	+ .01
.2458..	9.58	5	+ .04	+ .03	.0753..	11.33	7	− .04	− .04
.2306..	9.59	4	− .01	− .02	.0859..	11.14	5	− .02	− .02
.2200..	9.67	5	.00	.00	.0937..	10.97	5	− .05	− .04
.2106..	9.73	8	+ .01	.00	.1036..	10.88	8	+ .02	+ .02
.2007..	9.79	10	.00	.00	.1147..	10.73	8	+ .05	+ .04
.1911..	9.88	12	+ .02	+ .02	.1246..	10.56	12	+ .03	+ .02
.1817..	9.95	10	+ .01	+ .01	.1351..	10.39	14	.00	.00
.1718..	10.02	8	.00	.00	.1445..	10.31	11	+ .04	+ .04
.1615..	10.16	17	+ .04	+ .04	.1546..	10.13	10	− .02	− .02
.1506..	10.23	14	.00	.00	.1641..	10.10	11	+ .04	+ .03
.1396..	10.37	14	+ .01	.00	.1744..	9.97	10	.00	.00
.1311..	10.44	16	− .03	− .04	.1847..	9.90	9	+ .02	+ .01
.1212..	10.59	17	− .03	− .04	.1941..	9.79	9	− .02	− .03
.1121..	10.78	14	+ .01	.00	.2050..	9.71	8	− .02	− .03
.1013..	10.91	17	− .04	− .03	.2157..	9.71	6	+ .04	+ .03
.0906..	11.12	14	− .01	.00	.2242..	9.63	8	+ .01	.00
.0809..	11.30	10	− .02	− .02	.2345..	9.57	7	.00	− .01
.0715..	11.51	12	.00	.00	.2507..	9.50	7	.00	− .01
.0617..	11.69	10	.00	.00	.2708..	9.48	7	+ .03	+ .02
.0509..	11.88	7	.00	.00	+0.2811..	9.43	4	+0.02	0.00
.0313..	12.05	5	− .04	− .01					
.0169..	12.08	4	− .02	− .02	+0.94....	9.42	5	+0.02	+0.02
−0.0082..	12.07	7	− .03	− .03	1.90....	9.35	5	− .05	− .05
+0.0060..	12.16	5	+ .06	+ .06	2.04....	9.41	7	+ .01	+ .01
.0139..	12.09	4	− .01	− .01	2.67....	9.38	5	− .02	− .02
.0261..	12.03	5	− .07	− .04	3.04....	9.42	3	+ .02	+ .02
.0356..	12.02	6	− .03	.00	4.04....	9.44	6	+ .04	+ .04
+0.0460..	11.87	6	−0.05	−0.05	+4.48....	9.36	7	−0.04	−0.04

An independent solution for the "uniform" elements yielded results identical with those obtained by Russell, which are, therefore, adopted as final for this paper. The determination of the "darkened" k followed the method of the other assumption. The mean value, derived from 10 points along the free-hand observation curve (assumed symmetrical as usual), is 0.703, with an average deviation of ± 0.026. To determine the constants for the theoretical light-curve, Table IIx was entered with this value of k, and the resulting values of $\psi(k,a)$, for the fractions $a^{1}{}_{1}$ used in determining k were plotted against the corresponding values of $\sin^2\theta$. The intercept and the slope of the straight line that best represented the plotted points gave at once, by equation (9),[1] $A=0.0364$, $B=0.02525$. It was found that by plotting the points on a large scale the determination of A and B was remarkably definite. A least-squares solution, based on the residuals from the adopted straight line, gave negligible corrections for both uniform and darkened disks. The probable error of each quantity is about one unit in the fourth decimal place. The determination of A and B (upon which depends the theoretical light-curve and the remaining orbital elements) from the plot of equation (9) was adopted, therefore, as a suitable substitute for a least-squares adjustment for the other orbits here considered. Because of the lack of information concerning the secondary minimum, a correction to k was not included among the unknowns of the least-squares solutions. It might be noted that with a change in k of one or two hundredths an adjustment of A and B is possible that would give a light-curve nearly identical with that adopted, but greater alterations would begin to show unallowable residuals. Equation (9) and the relation $\theta=\frac{2\pi t}{P}$ were used with the constants found above to compute the theoretical curve. The deviations, O.$-$C.$_d$, in columns five and ten of the table of normals, refer to this computed curve. The theoretical "uniform" curve determined by Russell is in the fourth column below; and the difference between the two, U.$-$D., in thousandths of a day, is in the fifth.

[1] The equations and tables referred to throughout this paper are those of the preceding discussion, *Astrophysical Journal*, **36**, 239, 1912.

The last column contains the difference in the magnitudes, computed by the two curves, at a time midway between t_d and t_u.

COMPUTED LIGHT-CURVES FOR *W Delphini*

α^s_1	Mag.	t_d	t_u	U.–D.	Δm
1.00	12.100	0ᵈ016	0ᵈ028	+12	+0.02
0.99	11.985	.042	.043	+ 1	+ .03
0.98	11.884	.050	.049	− 1	− .02
0.95	11.624	.064	.064	0	.00
0.9	11.292	.081	.081	0	.00
0.8	10.835	.106	.106	0	.00
0.7	10.514	.127	.127	0	.00
0.6	10.266	.146	.146	0	.00
0.5	10.066	.166	.166	0	.00
0.4	9.896	.185	.185	0	.00
0.3	9.749	.206	.205	− 1	.00
0.2	9.620	.229	.227	− 2	− .01
0.1	9.505	.258	.252	− 6	− .01
0.0	9.400	0.309	0.292	−17	−0.01

The curves are sensibly coincident except near the beginning and end, and at these points the residuals in the table of normals show that the difference is in favor of the "darkened" curve. The tendency of the observations to fall below the best attainable theoretical "uniform" curve near the beginning and end of eclipse has been observed by Professor Dugan in two partial eclipses,[1] and I have found it quite common among both the total and partial eclipses investigated. The theory of darkened stars takes care of at least a part of this discrepancy.

Table III and equations (10) and (11) give the other "darkened" elements of the orbit of *W Delphini:* $i=86°\ 7'$, $r_1=0.241$, $r_2=0.170$. The stellar radii are expressed as usual in terms of the radius of the relative orbit. Since the loss of light at principal minimum is $2^{mg}.70$, the small bright star has 0.917 of the light of the system. The ratio of the mean surface intensities, $\frac{J_1}{J_2}$, is $\frac{1}{22}$—a considerable change from the relative brightness on the hypothesis of uniform disks, which is entirely due to the increase in the relative size of the smaller star. The depth of the secondary minimum, which has not been observed, would be nearly double the theoretical $0^{mg}.027$ required by the uniform brightness theory, and its precise measurement would be of considerable value. If we assume the components

[1] *Contributions from the Princeton University Observatory*, No. 1, 1911; No. 2, 1912.

equally massive, we find that the density of the brighter is 0.060, and of the fainter, 0.021, in terms of the sun's density. The detailed comparison of the two sets of elements and of the light-curves will be made later.

2. *S Cancri.*—The observations have been collected into 51 normal places, of which eight are composed of measures made clearly outside the limits of minima, two occur near the epoch of secondary minimum, and the remainder define the light variation of the primary. Wendell's value of the period was adopted, but his epoch of zero phase was $0^{d}.02$ too early. The phases of all the observations were corrected accordingly. From 29 observations, constant minimum light is fixed at $10^{mg}.093$, with a probable error of seven thousandths of a magnitude. Maximum light, from 63 observations, is $7^{mg}.977 \pm 0^{mg}.004$. If the orbit is circular, the mid-epoch of secondary minimum is at phase $4^{d}.7423$. Two normal points in the table below are within three hours of this, hence, well within the minimum. I believe their deviations from constant light

NORMAL MAGNITUDES OF *S Cancri*

Phase	Mag.	No. Obs.	O.−C.$_u$	O.−C.$_d$	Phase	Mag.	No. Obs.	O.−C.$_u$	O.−C.$_d$
	mg		mg	mg		mg		mg	mg
$-0^{d}4480$..	7.97	7	−0.01	−0.01	$+0^{d}1388$..	9.58	10	+0.02	+0.01
.4260..	8.03	8	+ .05	+ .05	.1546..	9.37	8	.00	− .01
.4056..	8.04	9	+ .06	+ .06	.1644..	9.29	7	+ .02	+ .01
.3804..	8.07	9	+ .08	+ .05	.1740..	9.18	6	.00	.00
.3560..	8.06	7	+ .03	+ .02	.1888..	9.05	8	+ .02	+ .01
.3368..	8.13	7	+ .04	+ .03	.2112..	8.87	10	+ .05	+ .04
.3143..	8.19	7	+ .01	.00	.2245..	8.71	7	.00	.00
.2942..	8.28	10	+ .02	+ .02	.2385..	8.58	10	− .02	− .02
.2741..	8.40	11	+ .03	+ .03	.2550..	8.46	7	− .02	− .02
.2565..	8.49	10	+ .01	+ .02	.2711..	8.34	9	− .05	− .04
.2360..	8.62	12	.00	.00	.2850..	8.26	8	− .05	− .04
.2209..	8.74	6	.00	.00	.2990..	8.21	7	− .02	− .02
.2026..	8.90	4	.00	.00	.3194..	8.09	7	− .05	− .06
.1819..	9.08	6	− .01	− .01	.3393..	8.05	9	− .03	− .04
.1642..	9.23	7	− .03	− .03	+0.3913..	7.95	4	−0.03	−0.04
.1425..	9.50	6	− .01	− .02					
.1264..	9.66	10	− .02	− .03	+0.43 ..	7.97	9	−0.01	−0.01
.1029..	9.92	10	+ .02	+ .02	0.58 ..	7.97	5	− .01	− .01
−0.0203..	10.07	9	− .02	− .02	0.69 ..	7.98	10	.00	.00
+0.0238..	10.11	9	+ .02	+ .02	1.30 ..	8.00	9	+ .02	+ .02
.0498..	10.12	11	+ .03	+ .03	2.39 ..	7.97	9	− .01	− .01
.0690..	10.08	10	− .01	.00	3.53 ..	7.98	10	.00	.00
.0850..	10.06	7	+ .02	+ .03	4.6387..	8.01	5	(+ .03)	(+ .03)
.0941..	9.99	7	.00	.00	4.7715..	8.03	5	(+ .05)	(+ .05)
.1039..	9.91	7	.00	.00	7.05 ..	7.99	6	+ .01	+ .01
+0.1209..	9.74	11	0.00	0.00	+8.17 ..	7.97	5	−0.01	−0.01

of $+0^{mg}.03$ and $+0^{mg}.05$, respectively, demonstrate the measurable existence of the secondary dip. The average deviation of the normals of maximum light is not quite $\pm 0^{mg}.01$. In the following table the mean magnitudes have been rounded off to the second decimal place, though in plotting the curves and determining the residuals the third place was used.

The range of variation at primary minimum is $2^{mg}.116$, hence the light, L_2, of the smaller bright star is 0.858 of the total light. In the usual way, for several fractions, α^{1}_{1}, of the light lost, corresponding values were successively determined of the magnitude, and of t, θ, $\sin^2 \theta$, $B\psi$, and ψ. Entering the two ψ-tables for k, adjusting the weights of the individual determinations to reflect the relative accuracy of all parts of the curve, and taking the mean, the result, with considerable definiteness, was $k_u = 0.370$, $k_d = 0.523$. The straight-line determination of A and B, and the further derivation of the orbital elements, gave for the "uniform" and "darkened" assumptions, respectively,

$$
\begin{aligned}
A &= 0.0208, & 0.0208, \\
B &= 0.01276, & 0.01267, \\
i &= 83^\circ\ 10', & 85^\circ\ 25', \\
r_1 &= 0.203, & 0.184, \\
r_2 &= 0.075, & 0.096, \\
\frac{J_1}{J_2} &= \tfrac{1}{44}, & \tfrac{1}{22},
\end{aligned}
$$

and the "equal-mass" densities, $\bar{\rho}_1$, $\bar{\rho}_2$, are

$$
\begin{aligned}
\bar{\rho}_1 &= 0.009, & 0.012, \\
\bar{\rho}_2 &= 0.178, & 0.084.
\end{aligned}
$$

The subscript 1 refers in all cases to the larger star. For the disks uniformly bright the secondary minimum, k^2L_1, should be two hundredths of a magnitude, and on the opposing hypothesis twice as deep. Existing observations are insufficient to distinguish, though the average error of Wendell's constant light observations suggests that such a refinement is not hopeless.

The above values of A, B, and k are used in computing the theoretical curves. Their representation of the observations is shown by the two columns of residuals in the table of normals.

The persistence of sign near the beginning and end of eclipse does not indicate a discrepancy between theory and observation, but rather indicates a small, real, and unaccountable asymmetry. The fit of the theoretical curves to the mean of the branches of the observation curve is nearly everywhere within the uncertainty of the normal points. It should be noticed that the remarkable "stand-still" in the ascending branch of the curve, so long credited on the basis of the uncertain eye estimates of the early observers of this star,[1] was an illusion only.

COMPUTED LIGHT-CURVES FOR *S Cancri*

α^2_1	Mag.	t_u	t_d	U.−D.	Δm
1.00	10.093	0ᵈ071	0ᵈ053	+18	+0.02
0.99	10.029	.087	.085	+ 2	+ .02
0.98	9.969	.096	.095	+ 1	+ .01
0.95	9.807	.114	.115	− 1	.00
0.9	9.581	.136	.136	0	.00
0.8	9.235	.168	.169	− 1	− .01
0.7	8.973	.194	.195	− 1	− .01
0.6	8.762	.219	.219	0	.00
0.5	8.585	.242	241	+ 1	.00
0.4	8.433	.265	.263	+ 2	+ .01
0.3	8.300	.287	.286	+ 1	.00
0.2	8.181	.312	.313	− 1	.00
0.1	8.075	.340	.344	− 4	− .01
0.05	8.025	.358	.366	− 8	− .02
0.00	7.977	0.386	0.413	−27	−0.01

3. *SW Cygni*.—The observations of this star are much fewer in number than those of the other three, but the higher accuracy of the work makes it of nearly equal importance. The principal minimum is thoroughly determined, but the value of maximum light, $9^{\text{mg}}_{\cdot}06$, must depend upon only eight observations; and, as in the case of *W Delphini*, there are no observations near the phase of the secondary minimum. Constant minimum light, depending on 29 observations, is $11^{\text{mg}}_{\cdot}720 \pm 0^{\text{mg}}_{\cdot}002$. There is a slight, though perhaps not real, lack of symmetry in the curve. No alteration of the period given by Wendell was necessary, but a shift of $-0^{\text{d}}_{\cdot}0044$ of the zero phase was made. The 192 observations are collected into the 38 normal points of the following table—the last two groups falling outside the minimum.

[1] Clerke, *Problems in Astrophysics*, p. 306, London, 1903.

NORMAL MAGNITUDES OF *SW Cygni*

Phase	Mag.	No. Obs.	O.−C.$_u$	O.−C.$_d$	Phase	Mag.	No. Obs.	O.−C.$_u$	O.−C.$_d$
	mg		mg	mg		mg		mg	mg
−0^d.2265..	9.28	4	+0.01	0.00	+0^d.0092..	11.73	5	+0.01	+0.01
.2075..	9.43	6	+ .04	+ .04	.0343..	11.68	4	− .04	− .04
.1849..	9.57	5	.00	+ .01	.0544..	11.63	4	− .09	− .07
.1681..	9.74	5	.00	+ .01	.0682..	11.53	4	.00	.00
.1538..	9.90	6	.00	.00	.0792..	11.32	5	+ .02	+ .02
.1434..	10.06	6	+ .02	+ .02	.0907..	11.05	4	+ .03	+ .03
.1352..	10.17	6	+ .02	+ .02	.1002..	10.81	5	+ .01	.00
.1276..	10.30	5	+ .03	+ .03	.1090..	10.62	8	.00	.00
.1217..	10.39	4	+ .02	+ .01	.1195..	10.40	7	.00	.00
.1141..	10.53	5	+ .01	.00	.1290..	10.23	4	− .02	− .02
.1038..	10.71	5	− .01	− .02	.1389..	10.09	6	− .01	.00
.0949..	10.89	3	− .02	− .02	.1537..	9.91	5	.00	.00
.0847..	11.12	3	− .04	− .04	.1750..	9.66	6	.00	.00
.0729..	11.39	3	− .04	− .04	.1965..	9.48	5	.00	.00
.0629..	11.63	3	− .01	.00	.2116..	9.34	5	− .02	− .02
.0537..	11.70	4	− .02	− .01	.2368..	9.22	6	.00	.00
.0410..	11.73	5	+ .01	+ .01	.2641..	9.12	8	+ .02	.00
.0254..	11.73	7	+ .01	+ .01	0.288 ..	9.07	3	+ .01	.00
−0.0098..	11.72	8	0.00	0.00	+1.76 ..	9.05	5	−0.01	−0.01

The average deviation of a single determination of k from the mean of ten was less than ± 0.03 for each of the limiting assumptions. The computations gave the following results:

	Uniform	Darkened
k	0.494	0.666
A	0.0430	0.04285
B	0.02636	0.02621
i	83° 41′	87° 28′
r_1	0.266	0.247
r_2	0.131	0.166
$\frac{J_1}{J_2}$	$\frac{1}{48}$	$\frac{1}{24}$
ρ_1	0.017	0.021
ρ_2	0.141	0.070

The smaller star has 0.914 of the light. The secondary minimum should be about $0^{mg}.02$ and $0^{mg}.05$, respectively. The light-curves below, and the residuals from them in the table above, show general agreement throughout the middle, and the characteristic disagreement at the extreme ends.

COMPUTED LIGHT-CURVES FOR *SW Cygni*

α^1_2	Mag.	t_u	t_d	U.−D.	Δm
1.00	11.720	0.056	0.052	+ 4	+0.01
0.99	11.611	.065	.065	0	.00
0.98	11.514	.070	.070	0	.00
0.95	11.258	.081	.081	0	.00
0.90	10.936	.094	.094	0	.00
0.8	10.485	.116	.116	0	.00
0.7	10.168	.134	.134	0	.00
0.6	9.922	.152	.152	0	.00
0.5	9.722	.170	.169	+ 1	+ .01
0.4	9.554	.187	.186	+ 1	.00
0.3	9.408	.205	.205	0	.00
0.2	9.280	.225	.226	− 1	.00
0.1	9.165	.248	.253	− 5	− .01
0.05	9.111	.263	.270	− 7	− .02
0.00	9.060	0.286	0.310	−24	−0.02

4. *U Cephei.*—The inclinations of the orbits in the three cases above approach 90° when the "uniform" theory is replaced by the other limiting solution—an inevitable result of the large increase of k. When the former requires the maximum inclination of 90°, that is, a central transit, it is obvious, from equation (11), which then may be written $\phi^1_2(k)=\frac{B}{A}$, that in order to keep the solution real on the assumption of complete darkening, the quantities k, and A and B cannot be determined independently. No degree of darkening can hope to improve the solution where the "uniform" assumption demands a central eclipse, and the most satisfactory work possible in such a case is a compromising adjustment of k and the curve elements, A and B, keeping the inclination, of course, at its maximum. The "uniform" orbit of *U Cephei* shows this characteristic, and for that reason is suitable to show a limitation in the application of the "darkened" method. Although the most observed of all the eclipsing stars I have studied, a satisfactory orbit for it has been one of the hardest to derive.

The sets of measurements during the principal minimum have been collected into groups that cover approximately equal intervals of time, but are of very different weights because of the bunching of observations on the steep parts of the curve. The 54 observations during the constant minimum phase show a non-symmetrical

tendency that persists throughout the entire primary minimum. A downward slant of the bottom of the light-curve with increasing time is the observed effect, which I believe may be real and due to the irregular luminosity of the dark companion. The slight asymmetry of *S Cancri* is similar, and a sloping bottom seems to be so common with stars of large range, and bears such a definite

NORMAL MAGNITUDES OF *U Cephei*

Phase	Mag.	No. Obs.	$O.-C._u$	$O.-C._d$	Phase	Mag.	No. Obs.	$O.-C._u$	$O.-C._d$
	mg		mg	mg		mg		mg	mg
-0^d2420..	6.82	6	+0.03	+0.03	$+0^d0958$..	7.82	33	0.00	−0.02
.2230..	6.84	4	+ .06	+ .05	.1056..	7.62	17	− .03	− .04
.2058..	6.88	4	+ .06	+ .06	.1159..	7.46	10	− .04	− .03
.1912..	6.91	5	+ .05	+ .06	.1262..	7.33	12	− .03	− .01
.1761..	6.93	5	− .01	+ .02	.1367..	7.25	7	.00	+ .03
.1584..	7.11	7	+ .04	+ .07	.1465..	7.13	11	− .03	.00
.1391..	7.22	8	.00	+ .02	.1574..	7.08	10	+ .01	+ .04
.1210..	7.46	5	+ .03	+ .04	.1661..	7.00	6	.00	+ .03
.1074..	7.65	7	+ .02	+ .02	.1761..	6.92	7	− .02	+ .01
.0955..	7.84	10	.00	− .01	.1865..	6.92	8	+ .03	+ .06
.0861..	8.02	19*	.00	− .02	.2007..	6.82	8	− .01	.00
.0763..	8.26	33	− .02	− .03	.2222..	6.82	7	+ .03	+ .03
.0659..	8.62	36	.00	+ .02	+0.2414..	6.79	4	+0.01	+0.01
.0571..	8.91	33	+ .01	+ .05					
.0490..	9.05	10	− .11	− .02	SECONDARY MINIMUM				
.0435..	9.16	7	− .02	.00	+1.2672..	6.80	11		
.0360..	9.17	13	− .01	− .01	1.2962..	6.85	13		
.0263..	9.14	10	− .04	− .04	1.3259..	6.85	14		
.0164..	9.19	8	+ .01	+ .01	1.3547..	6.86	12		
−0.0057..	9.19	8	+ .01	+ .01	1.3859..	6.88	8		
+0.0049..	9.15	4	− .03	− .03	+1.4352..	6.83	5		
.0154..	9.20	3	+ .02	+ .02					
.0262..	9.20	4	+ .02	+ .02	MAXIMUM LIGHT				
.0366..	9.24	4	+ .06	+ .06	+0.44....	6.78	5	0.00	0.00
.0438..	9.22	4	+ .05	+ .07	0.54....	6.81	5	+ .03	+ .03
.0490..	9.14	8	− .02	+ .06	0.81....	6.79	7	.00	.00
.0569..	8.94	27	+ .03	+ .07	0.87....	6.82	5	+ .04	+ .04
.0668..	8.60	51	+ .02	+ .03	0.95....	6.81	5	+ .03	+ .03
.0766..	8.28	59	.00	.00	1.01....	6.73	5	− .05	− .05
.0863..	8.02	53	0.00	−0.02	+1.93....	6.74	5	−0.04	−0.04

* Includes one half-weight observation.

relation to the asymmetrical tendencies of the remainder of the curve, that it is hardly probable the whole effect is subjective. The mean constant minimum light is $9^{mg}_{.}177 \pm 0^{mg}_{.}007$. The observations outside primary minimum at once indicate a secondary whose depth is about $0^{mg}_{.}07$, but the 63 observations within its possible limits are not sufficient to fix the mid-epoch accurately, nor the

shape and depth with much definiteness.[1] Thirty-seven observations are entirely clear of both minima and fix constant maximum light at $6^{mg}.784 \pm 0^{mg}.009$. The phases published by Wendell have been corrected for an error of the zero point of $-0^{d}.0015$.

The "uniform" k, on first determination, was 0.636 ± 0.012, but with the best obtainable values of the curve elements, $A = 0.0724$, $B = 0.0434$, and the maximum inclination, the value of k, restricted by equation (11), had to be reduced to 0.631 in order to make the solution real. The agreement of this solution with the observed curve is reasonably satisfactory as is indicated by the first column of residuals in the table above. The remaining elements of the adopted "uniform" system are: $r_1 = 0.324$, $r_2 = 0.205$, $\frac{J_1}{J_2} = \frac{1}{20}$, $\bar{\rho}_1 = 0.032$, $\bar{\rho}_2 = 0.126$, and the depth of secondary minimum should be $0^{mg}.049$.

From the same values of the ψ-function used to determine the "uniform" k, we can enter the other table and obtain 0.814 as a mean "darkened" k that represents the whole curve with equivalent exactness. Then entering Table II*ax* we find $\phi^{1}{}_{2}(k) = 0.710$, which should be equal to $\frac{B}{A}$ for a central eclipse. But this is not reconcilable with the quotient $\frac{B}{A} = 0.600$, of the last paragraph, necessary for the best representation of the observations. A smaller k gives a smaller quotient, but pulls the ends of the computed curve away from the observations. However, the far heavier weight of the middle part makes this adjustment preferable to changes of A and B. After a few trials the best values obtainable, on the assumption of complete darkening, for k, A, and B, were 0.687, 0.0724, and 0.0436, respectively. The other elements are: $r_1 = 0.319$, $r_2 = 0.219$, $\frac{J_1}{J_2} = \frac{1}{17}$, $\bar{\rho}_1 = 0.034$, $\bar{\rho}_2 = 0.104$, and the secondary minimum would be $0^{mg}.077$ in depth. The range of $2^{mg}.393$ indicates that regardless of the assumption as to the distribution

[1] Observations by Professor E. C. Pickering with the meridian photometer also indicate the existence of the secondary minimum. Shapley, *Astronomische Nachrichten*, **192**, 79.

of the luminosity the smaller star has 89 per cent of the system's light.

LIGHT-CURVES FOR *U Cephei*

α^1_1	Mag.	t_u	t_d	U.−D.	Δm
1.00	9.177	0.048	0.040	+ 8	+0.03
0.99	9.092	.052	.048	+ 4	+ .08
0.98	9.014	.054	.052	+ 2	+ .07
0.95	8.809	.060	.059	+ 1	+ .03
0.9	8.535	.068	.067	0	+ .01
0.8	8.134	.082	.083	− 1	− .02
0.7	7.842	.095	.096	− 1	− .02
0.6	7.613	.108	.108	0	.00
0.5	7.423	.121	.120	+ 1	+ .01
0.4	7.260	.136	.133	+ 3	+ .03
0.3	7.121	.150	.147	+ 3	+ .03
0.2	6.997	.167	.162	+ 5	+ .03
0.1	6.885	.187	.182	+ 5	+ .02
0.05	6.833	.200	.195	+ 5	+ .02
0.00	6.784	0.221	0.225	− 4	0.00

The apparently unsymmetrical position of the secondary minimum would indicate that the orbit of *U Cephei* is eccentric. The evidence is too uncertain, however, to warrant a solution for elliptic elements. The observations would allow the zero phase of secondary minimum to be as much as one-tenth of a day after the mid-epoch of constant light. Using equation (31) of Russell's second paper, we would find in that case $e \cos \omega = 0.06$ where e is the orbital eccentricity and ω the longitude of periastron counted from the ascending node. There is no evidence of the relative durations of the two minima, so we cannot hope to separate e and ω. André has found the values, $e = 0.113$, $\omega = 210°$, from a consideration of the supposed periodical variation in the length of the orbital period.[1] His investigation gave also, approximately, $r_1 = 0.5$ and $r_2 = 0.3$, in units of the radius of the orbit; but he states that the dark companion is the smaller[2]—an impossible condition for a range of over two magnitudes and a constant minimum phase one-fifth the duration of total light change. The elements derived by Blažko[3] are based upon the light-curve determined by Yendell, whose observations were made by the Argelander method. The depth of minimum is three-tenths of a magnitude less than that

[1] *Traité d'astronomie stellaire*, **2**, 240, Paris, 1900.

[2] *Op. cit.*, pp. 209, 215, 232.

[3] *Op. cit.*, p. 99.

measured by Wendell, and the difference between Blaˇko's "uniform" elements and mine is largely due to this difference in range of variation. From the closeness of the component stars we should expect to find a small effect of prolateness, but Wendell's observations in maximum light give no definite sign of it.

The two limiting sets of elements for each of the four stars are collected into the following table. The densities are in terms of the sun's density, and for each system the radius of the circular orbit is the unit of length.

	W Delphini		*S Cancri*		*SW Cygni*		*U Cephei*	
	Uniform	Darkened	Uniform	Darkened	Uniform	Darkened	Uniform	Darkened
k......	0.528	0.703	0.370	0.523	0.494	0.666	0.631	0.687
i......	83° 25′	86° 7′	83° 10′	85° 25′	83° 41′	87° 28′	90°	90°
r_1......	0.256	0.241	0.203	0.184	0.266	0.247	0.324	0.319
r_2......	0.135	0.170	0.075	0.096	0.131	0.166	0.205	0.219
$\frac{J_1}{J_2}$.....	$\frac{1}{40}$	$\frac{1}{22}$	$\frac{1}{44}$	$\frac{1}{22}$	$\frac{1}{43}$	$\frac{1}{24}$	$\frac{1}{20}$	$\frac{1}{17}$
$\bar{\rho}_1$......	0.017	0.021	0.009	0.012	0.017	0.021	0.032	0.034
$\bar{\rho}_2$......	0.118	0.060	0.0178	0.084	0.141	0.070	0.126	0.104
r_1+r_2..	0.391	0.411	0.278	0.280	0.397	0.413	0.529	0.538

The "darkened" solution, unrestricted, doubles the ratio of mean surface intensities, and, while not materially increasing the density of the large faint companion, reduces the density of the brighter star to about one-half that obtained on the assumption of uniform disks. This point is of importance in indicating that the average density of the A-type stars, computed on the limiting basis of uniform luminosity, may be in error by as much as 100 per cent. The average "uniform" density of the brighter component for the four stars is 0.141; the "darkened" average, 0.080; and for the fainter companion, 0.019 and 0.022, respectively. These densities are computed on the assumption that both stars have equal masses. But it is well known that the brighter component of a close double is regularly the more massive, and, as a consequence, the brighter star will generally be more dense, and the fainter less dense, than computed above. It is probable, then, that the computed "uniform" densities very nearly represent the real conditions—the unequal masses being compensated for by a considerable degree of darkening at the limb.

The sum of the "uniform" radii is increased slightly in all cases by the introduction of complete darkening, but the maximum change is only 5 per cent. The effect on k is relatively large; but while the radius of the larger star is decreased, that of the smaller is increased, and the distance separating the stars is not much lessened.

The general effects of darkening on the elements here deduced, contradict, in part, the results derived by Blažko.[1] But he simply makes use of the longer duration of light change, and has made a secondary ordinary solution with the beginning of eclipse sooner and the beginning of totality later than for the "uniform" case. This will obviously increase k, but also increases the radius of the larger star.

Finally, we will compare the relative accuracy with which the two computed curves represent the observations. Referring to the pairs of curves in the individual discussion of each star, we see that the run of differences, U.−D., is negative and large at the beginning of eclipse where $\alpha^1{}_1=0$, changes sign three times, becoming positive at the beginning of totality. That is, for darkened stars the eclipse begins sooner and the total phase begins later, as found by Blažko. The large values of U.−D. near the beginning and end of eclipse do not indicate a large separation of the curves, for at those points the light changes slowly with the time and the curves are nearly flat. The relative fit of the two is shown by the average deviations of the normal points in the table below. It is sufficient for this purpose to give each point equal weight, except for *U Cephei* where unit weight was given for every ten observations or fraction of ten.

AVERAGE DEVIATIONS OF NORMAL POINTS

Average Deviation for	*W Delphini*		*S Cancri*		*SW Cygni*		*U Cephei*	
	Unif.	Dark.	Unif.	Dark.	Unif.	Dark.	Unif.	Dark.
	mg	mg	mg	mg	mg	mg	mg	mg
Upper third.....	0.015	0.011	0.037	0.034	0.010	0.009	0.028	0.033
Middle third....	.022	.020	.016	.015	.015	.013	.012	.023
Lower third.....	.026	.019	.014	.015	.023	.019	.018	.029
Constant light..	0.029	0.029	0.009	0.009	0.01:	0.01:	0.027	0.027

[1] *Op. cit.*, p. 98.

For the three stars that are free from the central transit restriction, the "darkened" curves have a slight advantage throughout the whole course of variation. But as remarked before, there is practically no difference between the two curves in the middle third, which is usually the most heavily observed portion. A more searching test is afforded by taking the *mean* observed residuals from the two computed curves for each star, grouping the normal points of the preceding tables as follows:

1. Normals for which α^1_1 is less than 0.2. If the stars are darkened at the limb, the observed light should here be fainter than that computed on the "uniform" hypothesis.

2. Normals with α^1_1 between 0.2 and 0.98, for which the two hypotheses should give practically identical results. These observations are numerous and have been grouped in three divisions.

3. Normals for which α^1_1 lies between 0.98 and 1.00. For these the "darkened" curve should be sensibly above the "uniform" curve. The interval covered by these phases is so short that the number of observations is very small.

4. Observations during constant light at minimum. We thus derive the following summaries. The weights assigned represent simply the number of observations combined into all the normals used. The weights of the individual normals have been considered in forming these groups. The mean results for the first three stars have been combined with equal weights—the column headed "weight" representing here only the total number of observations.

For the first three stars the observations unquestionably deviate from the "uniform" curve in just the manner that might be expected to result from darkening at the limb. But the minute observable differences between a zero and a unit darkening show the futility of attempting to determine the degree of darkening in this way; however, it seems probable that in these stars (which are of spectral type A), the darkening is very considerable. Before anything very definite can be said about its amount, a better determination of the observed curves at the beginning and end of eclipse will be necessary, and also sufficient information concerning the maximum light and secondary minimum to enable the elimination of "reflection" and prolateness effects.

The best "darkened" curve which can be obtained for *U Cephei*, consistent with the condition of central transit, is not nearly as good as the "uniform" curve. The observed depth of secondary minimum, however, appears to be in better accordance with the hypothesis of darkening.

Part of Curve		Beginning or End		Upper Slope		Middle Slope		Lower Slope		Just Outside Totality		Constant Minimum Phase	
		Res.	Wt.	Res.	Wt.	Res.	Wt.	Res.	Wt.	Res.	Wt.	Res.	Wt.
W Delphini													
Descending Branch	U	+0.009	43	+0.017	61	−0.018	78	−0.006	53	−0.040	5	0.000	20
	D	.000		+ .017		− .023		− .004		− .010		.000	
Ascending Branch	U	+ .010	47	+ .005	49	+ .025	53	− .024	38	− .048	11		
	D	− .001		− .001		+ .022		− .021		− .018			
Mean	U	+ .010	90	+ .012	110	− .001	131	− .013	91	− .046	16	.000	20
	D	.000		+ .009		− .005		− .011		− .016		.000	
S Cancri													
Descending Branch	U	+ .047	39	+ .020	33	− .002	28	− .007	33	....	0	+ .011	29
	D	+ .034		+ .023		− .002		− .012		....		+ .011	
Ascending Branch	U	− .037	35	− .024	33	+ .026	31	+ .005	36	+ .002	24		
	D	− .040		− .021		+ .018		.000		+ .009			
Mean	U	+ .005	74	− .002	66	+ .013	59	− .001	69	+ .002	24	+ .011	29
	D	− .003		+ .001		+ .008		− .006		+ .009		+ .011	
SW Cygni													
Descending Branch	U	....	0	+ .011	26	+ .020	26	− .022	17	− .02:	4	.000	29
	D	....		+ .013		+ .017		− .024		− .01:		.000	
Ascending Branch	U	+ .008	17	− .004	21	− .006	25	+ .015	18	− .09:	4		
	D	− .003		− .004		− .003		+ .012		− .07:			
Mean	U	+ .008	17	+ .004	47	+ .007	51	− .003	35	− .055	8	.000	29
	D	− .003		+ .005		+ .007		− .006		− .040		.000	
Mean for all three stars	U	+0.007	181	+0.006	223	+0.006	241	−0.006	195	−0.033	48	+0.004	78
	D	−0.002		+0.005		+0.003		−0.008		−0.016		+0.004	
U Cephei													
Descending Branch	U	+ .040	25	+ .010	30	− .007	88	− .019	50	....	...	− .002	53
	D	+ .052		+ .013		− .007		+ .029		....	...	− .002	
Ascending Branch	U	+ .001	64	− .017	72	+ .006	163	+ .022	39	....	...		
	D	+ .024		− .024		+ .002		+ .068		....	...		
Mean	U	+ .012	89	− .009	102	+ .002	251	.000	89	....	...	− .002	53
	D	+0.033		−0.012		−0.001		+0.046		....	...	−0.002	

SUMMARY

1. Orbital elements are obtained for the eclipsing variables, *W Delphini*, *S Cancri*, *SW Cygni*, and *U Cephei*, upon the hypotheses of uniform brightness and of complete darkening.

2. The computed light-curves on the latter hypothesis are more satisfactory, evidently indicating the certain existence of considerable darkening at the limb in stars of spectral class A, but the difference between the two sets of curves is so small that the determination of the amount of darkening seems to be far beyond the power of the very best existing photometric observations. The beginning and end of eclipse and of totality are the only times when the light-curves differ perceptibly, and at these points the greatest differences are a few hundredths of a magnitude. For intermediate degrees of darkening computed curves will in general fall between those here derived, which may be considered limiting solutions, and all the orbital elements will likewise be intermediate.

3. Elements derived on the assumption of complete darkening will differ in general from those obtained on the uniform disk hypothesis as follows: k will be increased on the average by about 25 per cent, the larger star becoming smaller, the smaller larger; the distance separating the surfaces of the component stars will, however, remain practically unchanged; the density of the brighter star, whose light determines the spectrum, will be approximately one-half so great; the ratio of surface intensities, $\frac{J_1}{J_2}$, will be nearly doubled, that is, on account of the effect on the surface areas of the stars, the difference between the intensities per unit area will be lessened; the inclination of the orbit will approach more closely to 90°, and consequently, in the cases where the uniform disk solution requires a central transit (as for *U Cephei*), the solution for darkened stars will not always be an improvement.

Princeton University Observatory
August 6, 1912

BAND SPECTRA OF ALUMINIUM, CADMIUM, AND ZINC

By EMILY E. HOWSON

It is a well-known fact that the spectra of the arc in air and *in vacuo* differ materially in the number of the lines and in the comparative intensities of the same lines. When the arc of certain metals is under reduced pressure, bands appear in their spectra which are not present in the arc burning in air. The object of this paper was to measure, as accurately as possible, the wave-lengths of the lines in these bands; then, to test some of the formulae which have been suggested for the mathematical representation of bands and series. The spectra of aluminium and cadmium were used for this purpose and the results are recorded below.

APPARATUS AND MEASUREMENTS

To obtain the spectra *in vacuo* a vessel was used of the type described by Dr. Barnes[1] in a recent article. The spectra were photographed in the first order of a Rowland concave grating having a radius of fourteen feet and a dispersion of 3.639 Å to the millimeter.

The spectra of the metal to be examined and of iron were photographed on the same plate. To accomplish this, one electrode was iron and the other the metal or brass filled with metal. By this means both spectra were obtained at the same time without a shift of one relatively to the other. The iron and the metal lines overlapped along the center of the plate, and it was through this portion of the plate that measurements on the lines were made, by means of a Gaertner micrometer microscope reading to 0.001 mm. Three iron lines near the band under investigation were used as standards and the metal wave-lengths calculated from these. A mean was taken of several settings and two or more plates were measured to insure accuracy. The wave-lengths of the standard iron lines were taken from Kayser's[2] table.

[1] *Astrophysical Journal*, **34**, 154, 1911.

[2] *Ibid.*, **32**, 217, 1910.

ALUMINIUM

The band spectrum of aluminium has been observed by a number of investigators; as yet very few have drawn particular notice to the bands with heads at $\lambda\lambda$ 4241, 4260, 4288, and 4353. Basquin[1] observed them in a rotating arc in hydrogen and Barnes[2] found that they appeared very strongly in an arc *in vacuo;* both recorded the wave-lengths and gave their conclusions as to the origin of these bands. No attempt has yet been made to connect the lines of these bands by a formula. The difference in the wave-lengths of adjoining lines increases directly as the distance from the head. It was further found that in most cases the second differences were approximately constant. In consequence it seemed but right to conclude that, knowing the head of the band and certain constants, the wave-lengths of the remaining lines could be calculated.

Fowler[3] working with the bands which occur in the spectrum of magnesium found that they could be best represented by a formula of the type:

$$\lambda_m = a + bm + cm^2 ,$$

where a, b, c are constants for a band and m an integer representing the number of the line in the series. Much the same result was obtained in the case of the bands of aluminium, as will be seen in what follows.

The lines were measured as has been described, using three iron lines as standards. In some cases plates were used which did not contain iron lines. It was therefore necessary to use an aluminium line as standard, its wave-length having been carefully determined from the plates containing the iron spectrum. These standard aluminium lines, one selected in each band, were calculated from three iron lines, namely, λ 4250.129, λ 4250.789, and λ 4282.404, the average wave-lengths for the standards being λ 4244.024, λ 4261.668, λ 4287.113. It is well known that pressure produces a change in wave-length which is different in different substances, and for different lines of the same substance. The errors thus introduced into the standard lines by changes in the

[1] *Ibid.*, **14**, 8, 1901. [2] *Ibid.*, **34**, 159, 1911.

[3] *Phil. Trans. Roy. Soc.*, **209** A, 447, 1909.

wave-lengths of the iron lines might amount to as much as .005 Å, but the relative wave-lengths of the band lines would not be affected.

The following Table I gives the values of the wave-lengths of lines in the four bands which we have called α, β, γ, and δ. The line λ 4259.400 was so close to the following line that an accurate measurement of its wave-length was difficult, so the value, as obtained from the formula given below, has been recorded.

TABLE I

α Band	β Band	γ Band	δ Band
4241.193	(4259.400)	4280.545	4353.162
41.652	59.635	83.805	53.359
42.318	60.016	87.113	54.057
43.023	60.497	90.574	55.068
44.024	60.999	94.173	56.426
45.250	61.668	98.019	58.097
46.528	62.451	4301.997	60.449
48.005	63.382	06.218	61.081
49.617	64.463	10.712	62.047
51.317	65.759	15.428	63.348
53.205	67.112	20.504	65.018
55.178	68.732		67.058
57.416	70.566		69.488
	72.593		71.340
	74.871		74.961
	77.556		78.935
			81.660

The second differences are approximately constant for all the bands except for β. Here the third differences are constant as shown by Table II.

TABLE II

First Differences	Second Differences	Third Differences
0.283		
0.355	0.072	0.014
0.441	0.086	0.012
0.539	0.098	0.015
0.652	0.113	0.014
0.779	0.127	0.014
0.920	0.141	0.014
1.075	0.155	0.012
1.242	0.167	0.015
1.425	0.183	0.012
1.620	0.195	0.015
1.830	0.210	0.014
2.054	0.224	0.012
2.290	0.246	0.016
2.542	0.252	

In the δ band there are two subseries which seem to be closely related to each other on account of the agreement of their first and second differences as shown in Table III.

TABLE III

First Subseries		Second Subseries	
First Differences	Second Differences	First Differences	Second Differences
0.698		0.632	
1.011	0.313	0.966	0.334
1.358	0.347	1.301	0.335
1.671	0.313	1.670	0.369
2.352	0.681	2.040	0.370
		2.430	0.390

Several formulae such as the following were tried upon the bands given in Table I.

$$n_m = n_0 - \frac{N_0}{(m+\mu)^2},$$

$$\lambda_m = a + bm^2.$$

The one which gave the best results was

$$\lambda_m = a + bm + cm^2 + dm^3.$$

Four lines were thus necessary to obtain the values of the four constants. Two separate calculations were made for these constants the average of which is given in Table IV.

TABLE IV

Band	a	b	c	d
α	4241.193	0.3809	0.0900	−0.0008
β	59.400	0.2522	0.0289	0.0023
γ	80.515	3.2240	0.0314	0.0046

The following Table V gives the differences between the observed values (Table I) and the calculated values as obtained with the above formula having the constants given in Table IV. The positive sign means that the observed value is greater than the calculated one.

TABLE V

m	α	β	γ
0	±0	±0	+0.030
1	−0.011	−0.048	+0.030
2	+0.010	−0.022	−0.003
3	−0.101	+0.018	−0.019
4	−0.077	−0.011	−0.026
5	+0.002	−0.003	+0.024
6	−0.018	+0.001	+0.019
7	+0.012	+0.012	+0.040
8	+0.027	+0.018	±0
9	−0.001	+0.072	+0.009
10	+0.003	±0	
11	−0.030	±0	
12	+0.074	+0.004	
13		−0.023	
14		−0.035	
15		+0.108	

CADMIUM

The cadmium bands extending from λ 4300 to λ 4500 have been observed before this but no relationship between the lines has so far been recorded. Jones[1] working with cadmium vapor in a discharge tube observed them and describes two bands with heads at λ 4494 and λ 4299. Later Fowler and Payne[2] using an arc *in vacuo* and Morse[3] by means of a Wehnelt interrupter found traces of these bands. Gallenkamp[4] mentions four heads—the first between the two principal lines, the second at λ 4400, the third at λ 4200, and the last at λ 4000.

It was found impossible to use a rod of metallic cadmium as one electrode for it rapidly melted away at the temperature of the arc. It was therefore placed in a cavity in the lower electrode made of brass. The lines in the spectrum due to the brass were eliminated by comparing the plates obtained when both cadmium and brass were used with those obtained when brass electrodes alone were used.

The differences in the spectra of cadmium in the arc in air and *in vacuo* are shown on Plate XIV. Fig. 1 is the spectrum in air and Fig. 2 the same *in vacuo*. Four distinct bands can be readily seen in the second figure. By applying the method of second differences,

[1] *Wied. Ann.*, **62**, 30, 1897.

[2] *Proc. Roy. Soc.*, **72**, 253, 1903.

[3] *Astrophysical Journal*, **21**, 223, 1905.

[4] *Zeits. f. Wiss. Photogr.*, **5**, 299, 1907.

PLATE XIV

FIG. 1.—Cadmium arc in air

FIG. 2.—Cadmium arc *in vacuo*

it was found that each band consisted of one or more series. The measurements of the wave-lengths of these lines were carried out in the same way as described above. The iron lines used as standards in these measurements were, for the first and second bands, λ 4494.571, λ 4482.266, and λ 4476.055; for the third and fourth, λ 4307.908, λ 4299.243, and λ 4294.124. Table VI gives these values. The series are marked by the letters α, β, γ, δ, ϵ, and ζ.

TABLE VI

4510.033	4486.746 δ	4454.674 γ	4373.740	4279.872 ζ
09.488	86.370 γ	53.668 δ	68.177 δ	77.145
09.048 α	85.032 δ	52.382	65.716	76.634 ζ
08.907 β	84.518 γ	49.924 γ	60.119	76.181
08.628 α	83.071 δ	49.138 δ	57.507	73.743
08.288 β	82.325 γ	47.609	13.310 ϵ	73.111 ζ
07.953 α	80.898 δ	44.733 γ	12.982 ϵ	70.059
07.498 β	79.940 γ	44.448 δ	12.414 ϵ	69.325 ζ
07.017 α	78.265 δ	39.455 δ	11.534 ϵ	66.226
06.404 β	77.977	37.762	10.338 ϵ	65.173 ζ
05.696 α	77.224 γ	36.867	08.773 ϵ	62.087
05.005 β	75.394 δ	34.284 δ	06.948 ϵ	60.864 ζ
04.121 α	74.172 γ	32.353	04.844 ϵ	56.306 ζ
03.420 β	72.327 δ	30.289	02.390 ϵ	53.068
02.265 α	70.851 γ	28.813 δ	4299.673 ϵ	51.365 ζ
01.504 β	69.022 δ	26.925	97.535 ζ	48.183
4499.972 α	68.074	24.026	96.847 ζ	46.634
99.315 β	67.289 γ	23.080 δ	95.965 ζ	46.106 ζ
97.401 α	65.588 δ	17.114 δ	94.913 ζ	43.062
96.791 β	65.253	10.849 δ	93.582 ζ	40.645 ζ
91.838	63.394 γ	04.409 δ	92.018 ζ	34.860 ζ
91.622	61.860 δ	4397.708 δ	90.137 ζ	28.737 ζ
91.209 γ	60.639	90.719 δ	88.024 ζ	22.349 ζ
90.812 γ	59.198 γ	89.185	85.598 ζ	20.169
90.272 γ	58.366	83.471 δ	82.817 ζ	15.812 ζ
89.351 γ	57.871 δ	81.603	80.882	
88.088 γ&δ	56.951	75.938 δ	80.254	

The same formula as that used for the aluminium bands, viz.:

$$\lambda_m = a + bm + cm^2 + dm^3 ,$$

TABLE VII

Bands	a	b	c	d
α	4509.073	-0.28234	-0.13306	-0.00176
β	08.907	-0.41268	-0.14084	$+0.00039$
γ	4491.199	-0.07485	-0.18919	$+0.00264$
δ	88.075	-1.18740	-0.16340	$+0.00190$

TABLE VIII

m	α	β	γ	δ
0	+0.025	±0.000	−0.010	−0.013
1	+0.028	+0.066	+0.159	−0.020
2	+0.009	+0.023	+0.041	−0.059
3	−0.005	+0.008	−0.008	+0.023
4	+0.006	+0.023	−0.046	−0.078
5	−0.006	−0.050	+0.055	+0.026
6	−0.056	−0.059	−0.019	+0.085
7	+0.001	−0.064	−0.015	+0.080
8	−0.011	±0.000	−0.090	+0.060
9			+0.013	−0.050
10			−0.001	−0.099
11			+0.146	

was found the most satisfactory for these cadmium bands. The values of the constants a, b, c, d, for the α, β, γ, and δ bands are given in Table VII and the agreement between calculated and observed wave-lengths in Table VIII.

ZINC

In eliminating the brass lines from the spectrum of the brass and cadmium combined a fluting in the neighborhood of λ 4300 was found to appear on all the plates. By the same method of elimination as employed above, this band was found to be due to the zinc in the brass. As their wave-lengths were measured in connection with the cadmium work, they are recorded in the following Table IX. Those lines which appear to belong to a series are marked with the letter η.

TABLE IX

4300.959	4281.436 η	4254.396	4222.014
4297.322	78.328 η	49.609	21.653
97.541 η	77.806	44.579	18.121
95.965 η	74.909 η	39.315	14.136
94.687 η	70.997 η	37.658	09.874
93.135 η	67.156	35.919	09.188
91.430 η	63.127	33.094	05.277
89.329 η	58.857	30.226	00.454
86.987 η	58.310	28.002	4195.288
84.333 η	57.728	24.987	89.745

In conclusion I wish to thank Dr. Barnes for his assistance and suggestions which he so kindly made during the course of the work.

Bryn Mawr College
June 1912

OBSERVATIONS OF THE SPECTRUM OF *NOVA GEMINORUM* No. 2[1]

By WALTER S. ADAMS and ARNOLD KOHLSCHUTTER

The first observations of the spectrum of *Nova Geminorum* No. 2 were made by us on March 22, nine days after its discovery by Enebo, the delay being due to unfavorable weather and a somewhat late receipt of the announcement of its position. From that time until May 27, observations were continued as the weather and the time at the disposal of the spectrograph permitted.

All of the spectrograms were obtained at the 80-foot focus of the large reflector with the Cassegrain spectrograph. At first a single prism of 63° angle with a camera lens of 102 cm focal length was used, but after April 5 this lens was replaced by one of 46 cm focal length. With the latter lens and suitable tilt of the photographic plate it is possible to obtain good definition throughout the entire spectrum from $H\epsilon$ to $H\alpha$ with the exception of a limited region near $H\beta$. For purposes of close comparison, however, we have photographed mainly the region between λ 3900 and λ 5000, only two plates having been taken of the less refrangible portion. A list of the photographs follows:

Plate No.	Date	G.M.T.	Camera	Region
γ 1076	1912 March 22	17^h 28^m	Long	H–λ 5000
1083	23	17 21	Long	H–λ 5000
1087	24	15 36	Long	H–λ 5000
1089	28	16 24	Long	$H\beta$–$H\alpha$
1091	30	16 30	Long	$H\epsilon$–λ 5000
1102	April 3	17 09	Long	$H\epsilon$–λ 5000
1103	5	17 23	Short	$H\epsilon$–λ 5000
1104	6	15 51	Short	$H\epsilon$–λ 5000
1105	6	16 39	Short	$H\epsilon$–λ 5000
1118	22	16 15	Short	$H\epsilon$–λ 5000
1149	28	16 21	Short	$H\epsilon$–λ 5000
1185	May 5	16 08	Short	$H\epsilon$–λ 5000
1188	10	16 15	Short	$H\epsilon$–$H\alpha$
1201	27	15 50	Short	$H\epsilon$–λ 5000

[1] *Contributions from the Mount Wilson Solar Observatory*, No. 62.

In discussing the results obtained from the reduction of these spectra we shall consider the subject under several heads:

1. General characteristics of the spectrum and changes during the observations.
2. Radial velocity.
3. The hydrogen lines.
4. The helium lines.
5. Nebular lines.
6. Probable identifications.

I. GENERAL CHARACTERISTICS OF THE SPECTRUM AND CHANGES DURING THE OBSERVATIONS

The first spectrum of the *Nova*, taken on March 22, showed a strong continuous spectrum with many dark lines, some sharp and narrow and others broad and diffuse. At numerous places faint bright bands are present, in most cases accompanied by strong dark lines, usually double, on the more refrangible side. Apart from hydrogen the more prominent of these bands are due to parhelium. The hydrogen lines are represented by strong bright bands from 20 to 30 Ångströms wide with strong double absorption lines to the violet. Each of the bright hydrogen bands has strong maxima of about equal intensity at the two edges and between the two is a broad faint absorption band at least partially broken up into numerous narrow dark lines. The effect is very similar to that observed by Campbell and Wright in the hydrogen bands of *Nova Persei* and described by them in their well-known memoir.[1]

The most noticeable changes in the spectrum in the days immediately following March 22 were the decrease in intensity of the continuous spectrum, the rapid changes and disappearance of the absorption lines, the very marked alterations in the hydrogen absorption lines, and the rapid changes in the maxima of the bright hydrogen bands. On the photographs of March 23 and 24 the dark hydrogen lines are still strong and double. On March 28, however, they are much weaker and the bright band between them appears like a wing on the bright hydrogen lines. The red line

[1] *Astrophysical Journal*, **14**, 269, 1901.

$H\alpha$ shows the effect most strongly. The next spectrogram, obtained on March 30, again shows the strong absorption lines, but each is itself double, thus forming a set of four. On succeeding spectrograms the more refrangible component grows fainter and finally disappears as does the other after persisting somewhat longer.

The two chief maxima of intensity at the edges of the bright hydrogen bands, after remaining approximately equal from March 22 to March 30, show a great change after that time. On March 30 the violet maximum is decidedly broader and somewhat stronger, while on the succeeding spectrogram taken on April 3 the red component is much the more prominent. This continues to hold true to the end of our series of observations on May 27. Within the bands there are numerous changes in the secondary maxima as well.

The main feature of the later photographs of the *Nova* is the gradual change of the spectrum in the direction of the nebular spectrum, which is apparently characteristic of all *Novae*. It is marked chiefly by the following changes:

1. A steady decrease in the intensity of the continuous spectrum.

2. A corresponding increase in the intensity of numerous bright bands in the spectrum, many of which are characteristic of the spectrum of nebulae. The most important of these is the chief nebular line, λ 5007, which is first seen with certainty on April 6. It increases very rapidly after that time and on the last photographs in the latter part of May it is nearly equal to $H\beta$ in intensity and one of the strongest features of the spectrum.

The second nebular line, λ 4959, was first seen on a spectrogram of April 22 and from this time until the end of our series of observations it grew rapidly stronger. On April 28 it formed one of a nearly equal pair with the helium line λ 4922 but after that time it was much the stronger of the two.

Other lines which increased greatly in intensity toward the end of the series of observations were the well-known nebular lines λ 4364 and λ 4687. The former is seen as a heavy wing upon the red side of $H\gamma$ on photographs taken subsequent to April 22. The line λ 4687 of the principal series of hydrogen was first seen as a faint shading upon the red side of the very bright band

λ 4614–λ 4662. It rapidly grew stronger and on the last photograph is a well-marked feature of the spectrum.

The very complex region between λ 4600 and λ 4700 undergoes many changes. On the earliest photographs there is merely a trace of some faint bright bands in this region. Between March 24 and March 30, however, a strong double bright band develops extending from λ 4628 to λ 4670 with the centers of its components at λ 4643 and λ 4662. This band later grows in width and intensity, the width reaching a maximum about April 28 when the entire band extends from λ 4574 to λ 4681. Its intensity is about one-half that of the brightest part of $H\beta$. After this time the band begins to break up into components the brightest of which extends from λ 4622 to λ 4661, its center being at λ 4642. On our last spectrograms this band has an intensity nearly equal to that of $H\beta$. It evidently coincides with the line observed by Campbell in the spectra of nebulae at 464 $\mu\mu$. The changes of intensity during the interval March 22 to May 10 are shown by the curves of Plate XVII.

In giving the results of our measures we shall give the values for four groups of plates. The first consists of the three spectrograms γ 1076, γ 1083, and γ 1087 taken on March 22, 23, and 24. The second group consists of γ 1091–γ 1105, taken between March 30 and April 6. The third group includes γ 1118 and γ 1149, taken April 22 and April 28. The fourth group consists of the photographs taken after May 5.

The less refrangible region from λ 5050 to λ 6600 is considered separately. The wave-lengths given are corrected for radial velocity.

Owing to the very rapid changes in the spectrum there are some cases of apparent contradiction in the results given in a single column; for example, the center of a dark line nearly coincides with the center of a bright band. These are due to changes on the photographs the results of which are grouped, and so are only apparent. It is hardly necessary to say that it is impossible in all cases to distinguish between true absorption lines and dark spaces, as well as between bright bands and portions of the continuous spectrum. Thus complex regions such as λ 4550–λ 4700 may be analyzed in very different ways by different observers.

TABLE I

Portion of Line or Band	Observed Wave-Lengths for Different Plate Groups				Identification
	γ 1076 –γ 1087	γ 1091 –γ 1105	γ 1118 –γ 1149	γ 1185 –γ 1201	
Violet edge bright band	......	......	3882.7	3881.5	
Center dark band	......	......	3884.7	3885.2	
Center bright band	......	......	3891.3	......	*H* ζ band λ 3889
Red edge bright band	......	......	3899.7	3900.8	
Violet edge bright band	3925.0	......	......	......	K band
Narrow dark line	3933.9	......	......	......	*Ca* λ 3934
Red edge bright band	3948.5	......	......	......	
Center dark band or line	3950.5	3952.0	......	......	
Center faint bright band	3955.2	3954.4	......	......	
Center dark band or line	3959.0	3958.0	......	......	
Violet edge bright band	3960.9	3962.6	3960.8	3960.7	*H*ε band λ 3970
Center dark line	......	3966.0	......	......	λ 3951–λ 3981
Narrow dark line	3968.7	3968.6	3969.2	3967.8	*Ca* λ 3969
Center bright band	3970.7	3972.6	3971.2	......	
Center dark line	......	3973.4	......	......	
Center bright maximum	......	3977.6	3977.6	......	
Red edge bright band	3980.2	3981.9	3982.0	3981.8	
Center dark line	3984.1	3983.5	3982.6	......	
Violet edge bright band	......	......	3987.1	3986.0	
Center dark band	......	4003.6	......	......	
Red edge bright band	......	4009.0	4006.6	4007.6	
Red edge dark band	......	4018.2	4018.2	4018.8	
Center faint bright band	......	4035.0	4034.4	......	
Red edge bright band	......	......	4052.3	4052.0	
Violet edge bright band	......	4062.2	4061.5	4061.8	
Center dark band	......	4067.0	......	4066.3	
Center bright band	......	4067.9	......	......	Nebular band
Violet edge bright band	4069.7	......	......	......	λ 4069
Red edge bright band	......	4073.6	......	......	
Center dark band	4072.9	4075.1	......	4074.0	
Violet edge stronger bright band	4077.0.	......	......	......	Probably part of *H*δ band
Maximum in dark band	......	4078.6	......	......	
Violet edge strong dark line	4080.4	4081.1	......	......	
Center strong dark line	4082.5	4083.4	......	4084.0	
Red edge strong dark line	4085.0	......	......	......	
Center bright band	4086.6	4085.2	......	......	
Violet edge dark line	4088.9	4087.0	......	......	
Center dark line	4090.5	4089.0	......	......	
Violet edge bright band	4092.6	4092.8	4089.9	4090.2	*H*δ band λ 4102 λ 4081–λ 4113

TABLE I—*Continued*

Portion of Line or Band	Observed Wave-Lengths for Different Plate Groups				Identification
	γ 1076 −γ 1087	γ 1091 −γ 1105	γ 1118 −γ 1149	γ 1185 −γ 1201	
Maximum in bright band...	4096.0	......	......	4094.4	
Violet edge dark band......	4098.4	......	......	......	
Center dark line...........	......	......	......	4098.6	
Center bright band.........	4102.7	4103.7	4100.4	4102.6	
Center dark line...........	......	4101.8	......	......	
Center dark band..........	4104.2	4105.4	4105.2	4102.0	
Violet edge bright maximum	......	4105.6	......	......	
Center bright maximum....	......	......	4109.4	4108.0	
Red edge dark band........	4109.2	......	......	......	
Center dark line...........	......	4110.0	......	4110.7	
Center bright maximum....	4111.1	4110.1	4111.2	......	
Red edge bright band......	4113.1	4114.5	4114.6	4115.1	
Center dark line...........	......	4123.6	......	......	
Center dark line...........	4133.4	......	......	......	
Violet edge faint bright band	......	......	......	4135.9	
Center dark line...........	4153.6	4154.3	......	......	*He* band λ 4144
Red edge faint bright band..	......	4156.2	......	4157.8	
Center faint dark band.....	4160.4	4158.2	4160.4	......	
Center dark line...........	......	......	......	4168.0	
Center faint bright band....	4173.1	......	......	......	*He* λ 4169
Violet edge faint bright band	......	4180.9	......	4179.9	
Center bright band.........	......	4185.1	4182.3	......	
Center dark band..........	......	4191.6	......	......	
Red edge bright band......	4192.7	4190.4	......	......	
Center dark line...........	4196.7	4197.4	......	......	
Center dark line...........	......	4200.4	......	4198.8	
Center faint bright band....	4200.6	......	......	......	(H′ λ 4201)
Center dark line...........	......	4206.7	......	......	
Center faint dark line	4210.9	4209.2	......	......	
Violet edge dark band......	......	4210.7	......	4212.7	
Center dark band..........	4213.2	4214.2	4215.6	4213.3	
Center faint bright band....	4217.0	......	......	......	
Center dark line...........	4219.1	4220.2	......	......	
Center strong dark line.....	4222.5	......	......	4224.6	
Violet edge bright band.....	4224.0	4223.0	4225.8	......	
Violet edge bright band.....	......	......	......	4231.0	
Center bright band.........	4235.2	4236.0	4238.2	......	
Center bright band.........	......	......	......	4240.6	
Center dark line...........	......	4234.7	......	......	
Center dark line...........	4236.0	......	......	......	
Red edge bright band......	4246.5	4244.8	......	......	
Center dark line...........	4248.9	4247.7	4250.0	4248.6	
Red edge bright band......	......	4252.8	4252.6	4251.3	
Center dark band..........	......	4256.3	4255.1	4255.7	

TABLE I—*Continued*

Portion of Line or Band	Observed Wave-Lengths for Different Plate Groups				Identification
	γ 1076 –γ 1087	γ 1091 –γ 1105	γ 1118 –γ 1149	γ 1185 –γ 1201	
Violet edge bright band.....	......	4259.6	4258.4	4259.3	
Center dark line...........	......	......	4263.3	4263.5	
Center faint bright band....	4271.4	4269.7	4269.3	4269.4	Nebular band
Violet edge faint bright band	......	4275.6	......	......	λ 4265
Center dark line...........	4279.5	......	......	......	
Red edge bright band......	......	4280.0	4280.2	4280.0	
Center dark line...........	4283.4	......	4282.8	4281.8	
Center faint bright band....	......	4283.7	......	4285.6	
Center dark line...........	4289.1	......	......	......	
Violet edge bright band.....	4291.4	4292.3	......	......	
Red edge bright band......	......	4292.2	......	......	
Center dark line...........	......	4293.9	......	4294.4	
Center bright band.........	4294.8	......	......	......	
Violet edge bright band.....	......	4297.2	......	......	
Center dark band..........	4302.5	......	4303.4	4304.3	
Center bright band.........	......	4304.8	......	......	
Violet edge bright maximum	4305.5	4306.0	4305.6	......	
Center dark line...........	......	......	......	4306.6	
Center bright maximum....	4310.9	4309.5	......	......	
Center dark line...........	......	4313.0	......	......	(*Ti* λ 4313.0)
Red edge bright band......	......	4313.9	......	......	
Center dark line...........	......	4316.0	4315.6	......	
Red edge bright band......	4317.3	......	......	......	
Center dark line...........	......	4318.0	4317.5	4316.2	
Center strong dark line.....	4320.0	4319.8	......	......	
Violet edge bright band.....	4322.6	4321.9	......	......	
Center bright band.........	4324.5	4323.6	......	......	
Red edge bright band......	4325.9	4325.4	......	......	
Maximum in dark line......	......	4326.2	......	......	
Center dark band..........	4328.4	4327.8	......	......	
Violet edge bright band.....	4330.8	4330.4	4328.6	4329.4	*H*γ band λ 4341
Narrow bright maximum ...	4334.2	......	4334.4	4333.8	λ 4316–λ 4354
Dark line................	4335.0	4334.2	......	......	
Center bright maximum....	4335.5	4335.6	......	......	
Violet edge dark band......	4336.8	......	......	......	
Narrow dark line..........	4337.4	4337.4	4337.4	4336.9	
Dark line................	......	4339.8	......	4339.4	
Dark line................	4342.2	4343.6	......	4343.0	
Center bright band.........	4342.6	4343.7	4341.4	4342.0	
Center broad dark band....	4343.4	4343.3	......	4341.9	
Red edge dark band........	4349.8	4348.4	......	......	
Dark line................	4348.7	4350.8	......	......	
Center bright maximum....	4351.1	4350.9	4350.1	4350.5	
Strong narrow maximum....	......	......	......	4351.8	
Red edge maximum........	4353.9	4353.1	......	......	
Red edge bright band......	4353.4	4354.4	4354.4	4353.9	

TABLE I—*Continued*

Portion of Line or Band	Observed Wave-Lengths for Different Plate Groups				Identification
	γ 1076 $-\gamma$ 1087	γ 1091 $-\gamma$ 1105	γ 1118 $-\gamma$ 1149	γ 1185 $-\gamma$ 1201	
Dark line	4356.3	4355.8	4354.8	4354.6	
Center broad dark band	......	......	......	4361.6	
Center bright wing	4361.4	4359.5	......	......	
Red edge bright wing	4363.3	4365.2	......	......	
Dark line	4364.8	4365.1	......	4364.2	
Center bright band	......	......	......	4364.8	Nebular band
Dark line	......	4367.0	......	4368.2	λ 4364
Violet edge bright band	......	4368.8	......	......	
Dark line	......	4372.6	......	......	
Bright maximum	......	......	......	4373.2	
Violet edge bright band	4376.0	......	......	......	
Red edge bright band	......	......	4379.0	4377.1	
Bright maximum	4379.0	......	......	......	
Center dark band	......	......	4380.0	4380.9	
Bright maximum	......	4382.2	......	......	
Dark line	4384.4	4386.6	......	......	
Center bright band	4386.0	4386.0	......	4388.1	*He* band λ 4388
Dark line	4389.2	......	......	......	λ 4376–λ 4397
Center faint bright band	4391.3	......	......	......	
Red edge whole bright band	......	......	......	4392.2	
Dark line	4392.6	4392.6	......	......	
Red edge bright band	4395.4	4398.5	......	......	
Dark line	4397.2	......	......	......	
Dark line	4399.4	4399.7	......	4398.9	
Violet edge bright band	4401.2	......	......	......	
Dark line	4402.5	......	......	4403.7	
Violet edge bright band	......	4406.0	4405.8	4406.2	
Dark line	4406.4	......	......	......	
Maximum in bright band	......	4409.4	......	......	
Dark line	4415.7	4416.6	......	4415.9	
Center bright band	4416.5	4418.0	......	4417.8	
Dark line	......	4419.4	4418.2	......	
Dark line	4423.5	4423.0	......	......	
Bright maximum	......	4425.0	4424.7	......	
Red edge bright band	4428.2	......	4429.8	4428.8	
Dark line	4429.0	......	......	4430.0	
Center dark band	4432.3	4431.1	4432.7	4433.2	
Violet edge bright band	4435.4	......	4435.8	4435.8	
Center bright maximum	......	4438.4	......	......	
Center bright band	4442.6	4441.6	4442.1	4443.0	*He* band λ 4438
Violet edge dark band	......	4446.2	4448.1	4447.0	λ 4436–λ 4450
Strong dark line	......	4446.9	......	......	
Red edge bright band	4450.5	......	......	4449.8	

TABLE I—*Continued*

Portion of Line or Band	Observed Wave-Lengths for Different Plate Groups				Identification
	γ 1076 –γ 1087	γ 1091 –γ 1105	γ 1118 –γ 1149	γ 1185 –γ 1201	
Center dark band..........	4452.4	4452.2	4452.1	4451.3	
Maximum in dark band....	......	......	4455.0	4455.0	
Violet edge bright band.....	4455.6	4457.9	......	......	
Very strong dark line.......	4460.8	4460.3	4461.0	......	*He* band λ 4472
Violet edge bright band.....	4463.0	......	4461.5	4462.5	λ 4452–λ 4485
Bright maximum...........	......	4465.0	......	4465.0	
Dark line.................	4467.0	4467.2	......	4467.7	(*Fe* λ 4466.7)
Dark line.................	......	......	......	4471.2	
Center bright band.........	......	4473.3	4472.6	4473.8	
Dark line.................	4477.7	......	......	......	
Center bright maximum....	......	4480.6	......	4481.0	(*Mg* λ 4481.4)
Red edge bright band......	4486.5	4485.3	4484.6	4484.5	
Dark line.................	4487.2	......	......	......	
Dark line.................	4489.3	4488.8	......	4487.8	(*Ti* λ 4488.5)
Center dark band..........	......	4492.2	4491.0	4490.8	
Dark line.................	4495.5	4493.8	......	4494.3	(*Fe* λ 4494.7)
Violet edge bright band.....	4496.3	......	4495.6	......	
Red edge dark band........	......	4499.6	......	......	
Dark line.................	4501.5	......	......	4501.6	(*Ti* λ 4501.4)
Dark line.................	4505.2	4505.6	......	......	
Dark line.................	4508.1	4508.0	......	4506.8	(*Fe* λ 4508.5)
Violet edge bright band.....	......	4508.1	4507.0	4508.1	
Dark line.................	......	4510.2	......	......	
Dark line.................	4511.9	4512.9	......	......	
Violet edge stronger bright band..................	4512.4	4512.1	......	......	
Bright maximum..........	......	4517.0	......	4516.2	
Dark line.................	4518.9	4517.8	......	4517.2	
Center whole bright band...	......	4520.1	......	4520.5	
Dark line.................	4522.8	4522.1	......	......	
Center bright band.........	4522.8	4523.2	......	......	
Dark line.................	......	4525.5	......	4526.6	(*Fe* λ 4525.3)
Dark line.................	4529.0	4529.0	......	......	(*Fe* λ 4528.9)
Dark line.................	......	......	......	4532.0	
Red edge bright band......	4533.7	4534.2	......	......	
Dark line.................	4534.7	......	......	4535.2	
Broad dark line...........	......	4536.7	......	......	
Dark line.................	4537.6	4538.3	......	4538.6	
Red edge bright band......	......	......	......	4538.4	
Violet edge bright band.....	4538.7	4539.8	......	......	
Dark line.................	4543.8	4544.8	......	......	
Red edge bright band......	......	......	......	4546.6	
Dark line.................	4547.0	4547.0	......	......	
Center bright band.........	4552.4	4551.3	......	......	
Dark line.................	......	4551.6	......	......	
Dark line.................	4554.6	4555.0	......	......	
Red edge bright band......	......	4562.7	4564.7	......	

TABLE I—*Continued*

Portion of Line or Band	Observed Wave-Lengths for Different Plate Groups γ 1076 –γ 1087	γ 1091 –γ 1105	γ 1118 –γ 1149	γ 1185 –γ 1201	Identification
Narrow dark line	4562.5	......	......	......	
Maximum in dark line	......	4566.2	......	......	
Red edge bright band	4568.6	......	......	4567.0	
Center dark band	4569.1	4569.5	4570.2	4570.5	
Maximum in dark band	4571.9	4570.9	4573.2	4571.4	(*Ti* λ 4572.2)
Violet edge bright band	4573.3	4574.9	4573.7	4575.2	
Dark line	4575.8	4575.6	......	......	
Center bright band	......	4579.4	......	......	
Dark line	4580.9	4580.8	......	4579.9	
Center bright band	4585.7	4586.0	......	......	
Dark line	4586.7	4587.8	......	4585.5	
Center bright maximum	......	4594.8	......	......	
Dark line	......	4596.4	......	......	
Red edge bright band	4598.2	4597.9	......	......	
Dark line	......	4598.9	......	......	
Bright maximum	......	......	......	4600.1	(Nebular 459 $\mu\mu$)
Dark line	4601.0	4600.6	......	......	
Center bright band	......	4601.0	......	......	
Dark line	4603.3	4603.2	......	......	
Strong dark line	......	4605.1	......	......	
Red edge bright band	4606.3	......	......	......	
Dark line	4608.3	4607.8	......	......	
Center dark band	4610.2	4610.4	......	......	
Center bright band	......	4611.7	......	......	(Nebular λ 4610)
Violet edge bright band	4613.0	4615.5	......	......	
Dark line	......	4617.7	......	4616.4	
Violet edge bright band	......	4621.2	......	4618.4	
Center bright band	......	4622.0	......	......	
Dark line	4623.0	4621.2	......	......	
Violet edge stronger bright band	......	4622.5	4622.4	......	
Dark line	4624.3	4625.7	4626.6	4626.0	
Bright maximum	4627.4	......	......	......	
Center bright band	4631.4	4632.2	......	......	
Center dark band	4632.3	4633.9	......	......	
Center dark line	......	4636.3	......	......	
Bright maximum	4638.4	......	4636.4	......	
Center bright band	......	4640.7	......	4640.8	Nebular 464 $\mu\mu$
Center dark band	4643.0	......	......	......	
Center bright maximum	......	4643.4	4646.0	......	
Dark line	4646.2	4645.3	......	......	
Red edge bright band	4649.5	......	......	......	
Dark line	......	4651.6	......	4650.7	
Center bright band	......	4654.3	......	......	
Center dark band	4655.9	......	......	4657.0	
Violet edge bright band	4659.2	......	......	......	

TABLE I—*Continued*

Portion of Line or Band	Observed Wave-Lengths for Different Plate Groups				Identification
	γ 1076 –γ 1087	γ 1091 –γ 1105	γ 1118 –γ 1149	γ 1185 –γ 1201	
Center bright maximum	......	4661.9	......	......	(Nebular λ 4663)
Red edge bright band	......	4664.0	......	4662.4	
Dark line	......	4667.8	......	4667.0	
Center bright band	4667.4	......	......	......	
Center bright band	4672.8	......	......	......	
Dark line	4674.8	4675.2	......	......	
Violet edge bright band	......	......	......	4674.2	
Red edge bright band	4675.3	4675.0	......	......	
Center bright maximum	......	......	......	4678.4	
Dark line	4678.4	4679.2	......	4679.7	
Center bright maximum	......	4682.3	......	......	Nebular λ 4687
Red edge bright band	4683.4	4682.4	4680.8	......	λ 4674–λ 4700
Dark line maximum	......	4686.1	......	4685.8	
Center bright band	......	......	......	4687.1	
Violet edge bright band	......	4689.0	......	4685.8	
Center bright maximum	......	......	......	4694.8	
Dark line	4694.0	4693.0	4690.7	4692.6	
Bright maximum	......	4696.8	......	......	
Red edge bright band	......	......	......	4700.3	
Red edge bright band	......	4706.4	4708.6	......	
Center bright maximum	4709.9	4709.1	4707.5	......	
Dark line	......	4720.3	......	......	
Red edge faint bright band	......	4726.6	4725.1	4723.8	
Center faint bright band	4738.5	......	......	......	
Violet edge dark band	......	4744.0	......	......	
Maximum in dark band	4751.6	4752.1	4753.1	4751.6	
Red edge dark band	......	4756.2	......	......	
Dark line	4756.0	4756.2	......	......	
Dark line	4762.0	4762.4	......	......	
Red edge dark band	......	4765.2	......	......	
Violet edge faint bright band	......	......	4772.7	4771.9	
Dark line	4781.4	......	......	4782.2	
Dark line	......	......	......	4789.6	
Center faint bright band	......	4792.6	4793.8	......	
Dark line	......	4794.4	4794.6	......	
Center faint bright band	......	......	......	4804.1	
Violet edge dark band	......	4818.2	4817.6	4816.3	
Dark line	4824.7	4825.3	......	4826.0	
Center dark band	......	4828.9	......	4830.5	
Strong dark line	......	4833.2	......	......	*Hβ* band λ 4862
Violet edge strong dark band	4835.8	......	......	......	λ 4833–λ 4877
Dark line	......	4835.8	......	......	
Center narrow bright band	4837.2	4836.3	......	......	
Center strong dark line	4837.8	4837.9	......	......	
Violet edge bright band	......	4837.8	......	......	

TABLE I—*Continued*

Portion of Line or Band	Observed Wave-Lengths for Different Plate Groups				Identification
	γ 1076 –γ 1087	γ 1091 –γ 1105	γ 1118 –γ 1149	γ 1185 –γ 1201	
Dark line	......	4841.1	......	......	
Center bright band	......	4841.7	......	......	
Red edge dark band	4841.4	4841.5	......	......	
Dark line	......	4842.3	......	4842.8	
Center bright line	4843.6	4842.9	......	......	
Red edge bright band	4845.9	4845.8	......	......	
Center strong dark line	4847.6	4847.6	......	......	
Violet edge bright band	4849.9	4849.8	4847.0	4847.8	
Narrow bright maximum	......	4852.0	......	......	
Bright maximum	4854.1	4854.4	4853.4	4854.0	
Narrow dark line	......	4853.2	......	4852.2	
Bright maximum	......	4855.7	4856.4	......	
Dark line	......	4856.2	......	......	
Violet edge dark band	4856.9	......	......	......	
Center dark line	4858.1	4857.8	4858.5	4859.0	
Center whole bright band	4863.0	4864.0	4862.6	4863.0	
Center dark band	4863.7	4864.5	......	4862.1	
Maximum in dark band	......	4863.9	......	......	
Maximum in dark band	......	4866.6	......	4866.5	
Red edge dark band	4870.7	......	......	......	
Bright maximum	4871.6	4872.3	4870.9	4871.2	
Center strong bright maximum	4872.9	4873.5	......	......	
Red edge bright band	4875.9	4877.6	4877.7	4877.7	
Center bright wing	......	4883.0	......	......	Part of *H*β band
Dark line	4885.1	......	......	......	
Red edge bright wing	......	4888.6	......	......	
Dark line	4889.9	4890.1	......	......	
Center strong dark line	......	4896.9	......	4898.2	
Dark line	4900.5	......	......	4901.6	
Center bright band	4905.4	......	......	......	
Center dark band	4909.9	4909.1	4909.0	......	
Maximum in dark band	4911.2	......	......	......	
Violet edge bright band	4912.1	4911.2	......	4911.4	
Violet edge stronger bright band	4913.4	4914.1	4913.7	4912.7	*He* band λ 4922 λ 4901–λ 4938
Dark line	......	4915.7	......	......	
Center bright maximum	......	4917.5	......	......	
Dark line	4920.7	4919.8	4920.3	4921.2	
Center dark band	4925.9	4925.1	......	4923.7	
Center bright band	4925.8	4926.2	4926.2	4924.4	
Center stronger bright band	......	4927.4	......	......	
Red edge bright band	4938.1	4938.0	4938.3	4936.1	
Center strong dark line	......	......	4940.5	4940.7	
Violet edge bright band	......	......	4943.1	4945.8	
Center bright band	......	......	4959.0	4960.1	Nebular λ 4959
Red edge bright band	......	......	4976.3	4973.6	

TABLE I—*Continued*

Portion of Line or Band	Observed Wave-Lengths for Different Plate Groups				Identification
	γ 1076 –γ 1087	γ 1091 –γ 1105	γ 1118 –γ 1149	γ 1185 –γ 1201	
Strong dark line	......	......	......	4978.0	
Violet edge faint bright band	4980.3	......	......	......	
Center faint dark band	......	......	4980.0	4983.3	
Strong dark line	......	......	......	4985.3	
Violet edge bright band	......	4990.8	4991.2	4989.5	
Center bright band	......	4992.8	......	......	
Violet edge stronger bright band	......	4993.5	......	4992.5	
Center strong dark line	4994.7	......	......	......	
Center bright maximum	......	4996.1	......	4997.1	*He* band λ 5016
Red edge bright band	5001.9	5003.7	......	......	λ 4995–λ 5032
Dark line	5004.5	5003.8	......	5004.0	
Dark line	......	5007.2	......	......	
Violet edge bright band	5006.9	5010.3	......	......	
Center bright band	......	5007.0	5007.8	5007.1	Nebular λ 5007
Center stronger part of bright band	5012.5	5011.9	......	......	
Dark line	5014.3	5015.2	......	5011.7	
Red edge bright band	......	5020.2	5023.6	5022.5	
Center bright band	5019.3	5020.1	......	......	
Dark line	5023.0	5024.2	......	......	
Center bright maximum	......	5027.2	......	......	
Red edge bright band	5032.1	5032.8	......	......	
Violet edge bright band	......	......	......	5040.6	
Center faint bright band	......	......	......	5048.7	*He* band λ 5048
Red edge bright band	......	......	......	5060.1	λ 5041–λ 5060

Portion of Line or Band	Observed Wave-Lengths		Identification
	γ 1089	γ 1188	
Violet edge faint bright band	5160.4	......	
Center bright band	5172.5	5176.7	*Mg b* group
Red edge bright band	5183.5	......	
Center very faint bright band	5239.0	......	
Center faint bright band	5279.0	......	
Violet edge bright band	5308.3	......	
Center bright band	5319.4	......	
Red edge bright band	5332.5	......	
Center faint bright band	5379.1	......	
Violet edge bright band	5566.9	......	
Dark line	5577.2	......	

TABLE I—*Continued*

Portion of Line or Band	Observed Wave-Lengths		Identification
	γ 1089	γ 1188	
Center bright band	5580.4	......	
Red edge bright band	5591.5	......	
Violet edge bright band	5649.2	......	
Violet edge bright band	......	5666.7	
Center bright maximum	......	5676.2	
Center bright band	5680.8	5680.2	
Red edge bright band	......	5693.9	
Red edge bright band	5710.6	......	
Violet edge bright band	5743.1	5742.6	
Center faint dark band	......	5754.5	
Center bright band	5757.3	5755.9	Nebular λ 5752
Bright maximum	......	5765.7	λ 5743–λ 5770
Red edge bright band	5770.0	5770.0	
Violet edge bright band	5847.3	......	
Violet edge bright band	......	5864.7	*He* band λ 5876
Maximum in bright band	5870.1	......	λ 5847–λ 5909
Center bright band	5877.9	5878.1	
Dark line	5880.9	......	
Center stronger part of band	5885.7	......	
Red edge bright band	......	5891.2	
Dark line	5890.3	......	D_2 *Na* λ 5890
Dark line	5896.6	......	D_1 *Na* λ 5896
Red edge bright band	5909.4	......	
Center faint bright band	......	5942.3	
Violet edge faint bright band	5989.0	......	
Center faint bright band	6004.8	......	
Red edge bright band	6017.1	......	
Center faint bright band	6158.8	......	
Center faint bright band	6248.8	......	
Violet edge bright band	6287.7	6289.3	
Center bright band	6302.4	6304.7	Nebular λ 6301
Red edge bright band	6317.8	6320.3	
Violet edge bright band	6352.0	......	
Center bright band	6367.6	6370.0	
Red edge bright band	6382.0	......	
Violet edge bright band	6449.5	......	
Center bright band	6474.1	......	
Center bright maximum	6480.1	......	
Center bright band	......	6486.5	
Dark line	6502.0	......	
Red edge bright band	6509.0	......	
Dark line	6519.6	......	

TABLE I—*Continued*

Portion of Line or Band	Observed Wave-Lengths		Identification
	γ 1089	γ 1188	
Violet edge bright band	6529.7	......	
Center bright band	6536.9	......	Wing on *Hα* band
Red edge bright band	6543.0	......	
Dark line	6545.1	......	
Violet edge bright band	6548.3	6545.4	
Maximum in bright band	6555.3	......	*Hα* band λ 6563
Center bright band	6567.0	6569.4	λ 6545–λ 6585
Center dark band	6567.2	......	
Maximum in bright band	6578.6	......	
Red edge bright band	6585.2	......	
Center bright wing	6593.7	......	
Red edge bright band	......	6595.2	
Red edge bright wing	6600.5	......	Part of *Hα* band
Bright maximum	......	6672	
Center faint bright band	......	6677	*He* λ 6678

2. RADIAL VELOCITY

The principal lines available for the determination of the radial velocity of the *Nova* are the narrow absorption lines H and K of calcium, certain faint lines, for the most part due to iron, which appear on some of the plates, and the narrow lines D_1 and D_2, which are present upon one of the photographs taken in the less refrangible region. Owing to the strong absorption of the glass of the prism employed, the spectrograms are rather weak in the H and K region and the results obtained from these lines are not very accordant. The following is a summary of the values from the various lines:

Plate	Lines	Velocity	Reduction to Sun	Radial Velocity
		km	km	km
γ 1076	H	+40.2	−29.3	+10.9
1083	H, K	+47.0	−29.4	+17.3
1087	H, K	+33.1	−29.3	+ 3.8
1104	H	+35.0	−29.4	+ 5.6
1118	H	+28.5	−27.5	+ 1.0
1089	D_1, D_2	+47.4	−29.5	+17.9
1076	4222, 4528	+47.3	−29.3	+18.0
1083	4222, 4236, 4528	+39.6	−29.4	+10.2
1087	4222, 4250, 4494, 4501, 4528	+35.2	−29.3	+ 5.9

Although the range shown by these observations is rather large, in view of the character of the lines we do not consider any certain variation of velocity as established. The mean of the results as given in the table is

+10 km

and the mean of the final results of the six plates is

+10 km.

Determinations of the radial velocity by other observers are as follows:

Curtiss.........+ 9 km
Plaskett........+12 km with a probable variation of 15 km
Küstner........+ 7.0 km

3. THE HYDROGEN LINES

The bright hydrogen bands are characterized by definite edges upon the red side which can be measured with a very fair degree of accuracy. On the violet side the dark absorption lines upon the

CENTERS OF BRIGHT HYDROGEN BANDS

Plate	$H\epsilon$	$H\delta$	$H\gamma$	$H\beta$	$H\alpha$
γ 1076	3971.0	4103.2	4342.4	4863.0	......
1083	3970.1	4102.5	4343.3	4862.8	......
1087	3970.7	4102.3	4342.2	4862.9	......
1089	......	......	......	4862.9	6566.8
1091	3972.5	4102.7	4342.2	4863.1	......
1102	3972.5	4102.3	4342.8	4863.5	......
1103	......	4103.0	4343.1	4863.9	......
1104	3972.7	4104.7	4343.1	4867.9	......
1105	......	4105.8	4343.9	4864.6	......
1118	3972.0	4103.0	4342.2	4862.7	......
1149	3970.6	......	4340.9	4862.5	......
1185	3971.2	4103.2	4341.3	4862.4	......
1188	......	4101.9	4341.9	4863.0	......
1201	......	4103.4	4342.4	4863.3	......
Mean	3971.5	4103.2	4342.4	4863.3	6566.8
Δ	+1.3	+1.3	+1.8	+1.8	+3.8

earlier photographs form the boundary which seems to persist as the absorption lines grow fainter. These two limits, accordingly, represent the principal part of the emission band, while a broad fainter band extends toward the violet. The strong band is the

portion upon which our measures of width and displacement have been made. In the accompanying tables we have collected the results of our measures upon both the dark and the bright hydrogen lines.

An examination of the measures of the bright hydrogen bands shows that as in the case of *Nova Persei* the centers are displaced toward the red. On our photographs we have measured the centers directly, as well as the violet and the red edges of these bands. Accordingly, two independent determinations are available. Collecting all of the results we obtain the table on p. 308.

The displacements from the normal positions of the lines are given opposite Δ in the last row of the table. It is a peculiar fact that these values are better satisfied by a law in which the displacement is directly proportional to the square of the wave-length than they are by one in which it is proportional to the first power such as is found for the dark hydrogen lines and the widths of the bright hydrogen bands. The difference is due almost entirely to $H\alpha$ for which but one determination is available. A least-squares solution gives the following residuals in the two cases:

	λ	λ^2
$H\epsilon$	−0.2	0.0
$H\delta$	−0.2	−0.1
$H\gamma$	+0.2	+0.2
$H\beta$	0.0	−0.1
$H\alpha$	+1.3	+0.2

The dark hydrogen lines could be measured satisfactorily upon but a few of the earlier spectrograms. The results follow:

DARK HYDROGEN LINES

Plate	$H\epsilon$		$H\delta$		$H\gamma$		$H\beta$		$H\alpha$
	I	II	I	II	I	II	I	II	I
γ 1076	......	......	4090.2	4082.2	4328.3	4319.5	4847.6	4837.0	......
1083	3959.0	3950.5	4090.6	4082.4	4328.4	4320.2	4847.5	4837.5	......
1087	3958.9	3950.5	4090.8	4082.8	4328.5	4320.4	4847.7	4839.0	......
1089	......	......	......	......	......	......	4848.0	......	6545.2
Mean	3959.0	3950.5	4090.5	4082.5	4328.4	4320.0	4847.7	4837.8	6545.2
Δ	−11.2	−19.7	−11.4	−19.4	−12.2	−20.6	−13.8	−23.7	−17.8

If we take the values of the displacements of the dark lines, given as Δ in the table, and determine their variation with wave-length we find the relationship obtained by Campbell and Wright for the dark hydrogen lines in *Nova Persei*, and by Plaskett in the case of the present *Nova*—that is, the displacement is directly proportional to the first power of the wave-length. The residuals from a least-squares solution assuming the values of equal weight are as follows:

	Component I O.−C.	Component II O.−C.
$H\epsilon$	+0.2	+0.5
$H\delta$	0.0	−0.4
$H\gamma$	+0.1	−0.4
$H\beta$	+0.4	+0.3
$H\alpha$	−0.4	.....

These residuals are within the limits of error of the measurements.

We have already referred to the fact that on plate γ 1091 taken March 30 each component of the hydrogen lines is itself double, although in the case of $H\delta$ and $H\beta$ we have been unable to measure the separate portions of the less refrangible component. The values for this plate are as follows:

	$H\delta$			$H\gamma$				$H\beta$		
	I	II		I		II		I	II	
		a	*b*	*a*	*b*	*a*	*b*		*a*	*b*
γ 1091....	4088.9	4078.6	4082.2	4326.2	4328.5	4315.9	4319.8	4846.5	4833.2	4837.9
Separation		3.6		2.3		3.9			4.7	

The values of the separation of the two lines forming component II appear to be closely proportional to the wave-length. It is a noteworthy fact that the position of the *b* line of component II in each case occupies the same position as the center of the whole component upon the plates γ 1076–γ 1089. In other words, the doubling of the lines upon γ 1091 is due to a new component formed about 4 Ångströms to the violet of the original lines. The change,

accordingly, can hardly be ascribed to anything in the nature of a variation of pressure or to a possible magnetic field, but must rather be due to the action of an additional mass of absorbing gas, and it is probably allied to some of the phenomena of multiple reversal in laboratory spectra.

The widths of the bright hydrogen bands are, of course, influenced by the density of the spectrograms, and similarly the relative widths are affected by the curve of sensitiveness of the photographic plates employed. A comparison of the widths of the lines for the whole series of photographs is of considerable interest, however. In the accompanying table the values are given in Ångström units. Owing to a defect in the photograph at the position of the $H\alpha$ line on γ 1188, its value is omitted.

WIDTHS OF BRIGHT HYDROGEN BANDS

Plate	$H\epsilon$	$H\delta$	$H\gamma$	$H\beta$	$H\alpha$
γ 1076.......	18.7	20.8	22.5	26.1	....
1083.......	19.3	20.8	....	26.9	....
1087.......	20.2	19.9	22.4	25.7	....
1089.......	....	....	....	26.3	38.8
1091.......	22.7	23.0	22.0	27.2	....
1102.......	....	24.5	25.6	29.0	....
1103.......	....	24.1	24.0	28.5	....
1104.......	17.4	20.1	23.2	28.5	....
1105.......	....	17.2	22.1	28.2	....
1118.......	20.5	22.0	25.8	29.6	....
1149.......	22.1	27.1	25.7	31.9	....
1185.......	21.0	25.6	25.4	32.1	....
1188.......	....	25.0	24.6	30.1	....
1201.......	....	23.1	22.8	24.8	....
Mean......	20.2	22.3	23.8	28.2	38.8

An investigation of these values shows that, like the displacements of the hydrogen absorption lines, they vary in direct proportion to the wave-length. The residuals given by a least-squares solution assigning weights according to the number of measures are as follows:

	O.-C.
$H\epsilon$..............	-1.8
$H\delta$..............	-0.5
$H\gamma$..............	-0.3
$H\beta$..............	$+1.2$
$H\alpha$..............	$+2.4$

A similar relationship has been found by Professor Plaskett for the widths of the bright hydrogen bands.

4. THE HELIUM LINES

The helium and parhelium lines which can be identified with reasonable certainty in the *Nova* spectrum are given in the following list. The absorption lines accompanying the bright bands are also included, the more doubtful identifications being placed in parentheses.

CENTERS OF HELIUM LINES

He	Bright Band	Absorption Lines I	Absorption Lines II
4143.92	4146.4	(4133.4)	(4123.6)
4169.13	4173.1	......	......
4388.10	4387.4	......	......
4437.72	4438.4	(4429.5)	(4418.6)
4471.65	4473.2	4460.6	(4452.2)
4922.10	4925.9	4911.1	4900.6
5015.73	5019.5	5004.2	4994.7
5047.82	5048.7	......	......
5875.87	5878.0	......	......
6678.37	6677	......	......

In addition to these lines λ 4713.25 is probably present, at least upon the later photographs, but blended with a portion of the great band which extends from λ 4600 to beyond λ 4700. The average displacement of the bright bands toward the red is 2.1 Ångströms, or about the same as that of the hydrogen lines, but the measurements are much less accurate except in the case of λ 4926 and λ 5020, the bands being fainter and probably complicated with other bands in some cases. It seems probable that the displacements of both dark and bright lines are proportional to the wave-length.

Campbell and Wright in their discussion of the spectrum of *Nova Persei* have called attention to the interesting fact that on the earlier spectrograms of the star the parhelium lines are the ones observed, while in the later observations these have become very faint or have disappeared and the helium lines have become prominent. They refer to the observations of Runge and Paschen which indicate that with increase of pressure in the radiating gas the

helium lines become stronger relatively to the parhelium lines. Of the lines listed in the table above as observed in *Nova Geminorum*, λ 4471, λ 4713, and λ 5875 belong to the helium series and the remainder to parhelium. The line λ 4471 was probably present upon the earliest photographs, but very faint. It was first measured by us on a spectrogram taken on April 6, and continuously throughout the series after that time. The line λ 4713 we have already referred to as probably being present upon the later photographs merged in another bright band. The D_3 line, λ 5876, is present on the spectrogram of March 28, but is considerably stronger upon the photograph of May 10. The parhelium lines, with the possible exception of λ 5048 and λ 6678, were much stronger upon the earlier photographs, although most of them could still be seen throughout the whole series. The line at λ 5016 was last measured on March 30. The two parhelium lines, λ 5048 and λ 6678, however, appear to be present only upon the later photographs, the former being first measured on the spectrogram of May 5, and the latter on May 10. In general the relative behavior of helium and parhelium lines seems to resemble their behavior in *Nova Persei*, but not to be identical with it.

5. NEBULAR LINES

The bands which are almost certainly identical with lines observed in the spectra of nebulae are indicated in Table I. In addition to hydrogen and helium they are as follows:

Nova		Nebulae
Limits	Center or Maximum	
4062–4074	4068	4069
4259–4280	4270	4265
....	4365	4363
....	4579	4574
....	4599	459
....	4612	461
....	4641	464
4674–4700	4687	4686
4954–4974	4960	4959
4993–5022	5007	5007
5743–5770	5757	5752
6288–6319	6303	6301

The line λ 4686 is the first line in the principal series of hydrogen. The three lines of the second subordinate series may perhaps be present in the *Nova* spectrum; they are known to be present in the spectra of Wolf-Rayet stars, and their wave-lengths as determined by us in the star $BD+30^\circ$ 3639 are added for comparison.

H	*Nova*	$BD+30^\circ$ 3639
4026...........	Band 4018–4052	4028
4201...........	Center faint band 4201	4201
4542...........	Violet edge bright band 4540	4542

The spectrum of the *Nova* in its later stages and the spectra of Wolf-Rayet stars have numerous features in common. The greatest point of difference is, of course, the absence, or at least the comparative faintness, of some of the principal nebular lines in the Wolf-Rayet spectrum. Apart from this feature there is probably fully as much difference between spectra of individual stars of the Wolf-Rayet type as there is between the *Nova* and certain of these stars. For purposes of comparison the spectrum of the Wolf-Rayet star $DM+37^\circ$ 3821 is reproduced with the *Nova* spectra in Plate XV. The most striking feature of the spectrum of this star is the great intensity of λ 4686 and the prominence of the three lines already referred to which belong to the second subordinate series of hydrogen, λ 4026, λ 4201, and λ 4542.

A comparison of the widths of the bright hydrogen bands in the spectrum of $DM+37^\circ$ 3821 and of the *Nova* gives the following results:

	Nova	$DM+37^\circ$ 3821
$H\delta$..................	λ 4092–4114	4081–4117
$H\gamma$..................	4330–4354	4325–4354
$H\beta$..................	4849–4876	4843–4877

Within the limits of error of measurement the red edges of the bands have the same position. The violet edges in the case of the *Nova* are affected by the presence of absorption which is absent in the case of the Wolf-Rayet stars. The violet edges, accordingly, differ by roughly the same amount in the two cases. It is clear, therefore, that in a type of spectrum which we are accustomed to

PLATE XV

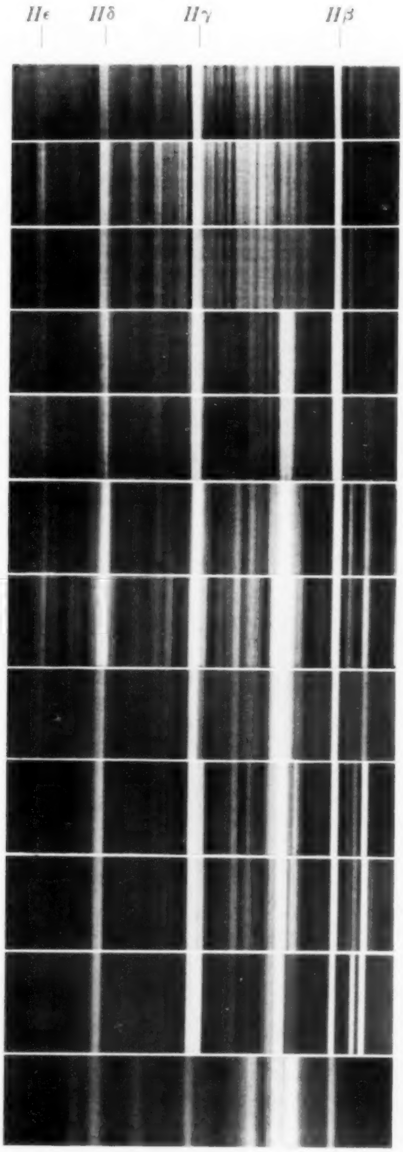

1 March 22, 17^h 28^m

2 March 23, 17^h 21^m

3 March 24, 15^h 36^m

4 March 31, 18^h 6^m

5 April 3, 17^h 9^m

6 April 6, 15^h 51^m

7 April 22, 16^h 15^m

8 May 3, 16^h 24^m

9 May 5, 16^h 8^m

10 May 10, 16^h 15^m

11 August 19, 0^h 10^m

12 *D.M.* $+37°$ 3821

1–11 Spectra of *Nova Geminorum* No. 2

12 Spectrum of Wolf-Rayet Star *D.M.* $+37°$ 3821

consider as relatively permanent, emission bands of the same order of width are present as in the spectra of *Novae*. On the other hand, the hydrogen lines in the spectrum of the Wolf-Rayet star $BD+30°$ 3639 are very narrow while other bands in the spectrum are as much as 20 Ångströms wide. This seems to us an objection to the hypothesis of Kayser that such bands may be due to the Doppler effect in gases under the bombardment of *Kanalstrahlen*.

In 1907 Hartmann made an important investigation of the spectrum of *Nova Persei* nearly six years after its discovery[1] and found its spectrum to resemble very closely that of the Wolf-Rayet star $BD+35°$ 4001. *Nova Persei* at that time was of about the eleventh magnitude.

6. PROBABLE IDENTIFICATIONS

The sodium lines D_1 and D_2 appear as narrow absorption lines in a bright band whose red edge falls at λ 5910. On the violet side this band blends with the bright D_3 band of helium.

A faint bright band extending from λ 5160 to λ 5184 is probably due to the *b* group of magnesium. A maximum at λ 4480 in the bright helium band λ 4463–λ 4485 is probably due to magnesium λ 4481.

The H and K lines of calcium like the sodium lines are narrow absorption lines in broad bright bands. The bright band due to the K line extends from λ 3925 to λ 3949, while the H band is lost in that of the $H\epsilon$ line. The K band is not seen after March 30. It seems very doubtful to us whether λ 4227 of calcium is represented in the *Nova* spectrum. This region is extremely complex and the bright band falling nearest the position of the line extends from λ 4224 to λ 4246 with a center at about λ 4235 on the earlier plates. On later photographs it seems to have even a longer wave-length, due probably to an extension of the band toward the red. The two absorption lines λ 4223.1 and λ 4213.9 probably belong to this band, and the wave-lengths of all three make it improbable that this can be due to calcium λ 4227.

A number of faint absorption lines present on the earliest plates may perhaps be identified with calcium. A number of

[1] *Astronomische Nachrichten*, **177**, 113, 1908.

these are given by Professor Küstner. Our own values are as follows:

Nova	Sun (Rowland)
λ 4282.1	4283.17
4302.8	4302.69
4307.3	4307.91
4459.0	4454.95
4580.7	4581.58
.4587.0	4586.05
4685.9	4685.45

In view of the large number of dark lines present in the *Nova* spectrum these identifications seem to us of rather doubtful value.

A considerable number of the absorption lines may be identified with lines of iron, and several others with lines of titanium, particularly with enhanced lines of this element. The possible identifications are indicated in Table I.

In his discussion of the spectrum of *Nova Lacertae*[1] Mr. Wright has instituted an interesting comparison between the bright stellar bands and the lines of the spark spectrum of nitrogen. Other observers have noted a similarity between the spectra of Wolf-Rayet stars and the spectra of oxygen and nitrogen. If we compare the lines of nitrogen given by Wright with our measures of the bright bands of *Nova Geminorum* we obtain the list in Table II.

There is practically a continuous band in the *Nova* spectrum between λ 4600 and λ 4700, and the values given are the centers of subordinate bands or of maxima. The fainter lines of the nitrogen spectrum show about the same degree of agreement with the stellar bands. In view of the evidence we are inclined to consider the presence of nitrogen in *Nova Geminorum* as probable, although we would agree with Mr. Wright in considering it as hardly proven.

The announcement by Professor Küstner and Dr. Giebeler of the discovery of dark lines in the *Nova* spectrum due to radium and the radium emanation arrived while we were engaged in preparing our results for publication. Owing to the fact that our series of observations did not begin until March 22, or several days after the first observations at Bonn, the results are not fully comparable, especially in view of the very rapid changes in the spectrum at

[1] *Lick Observatory Bulletin*, No. 194, 1911.

this time. As bearing on the question of the presence of radium absorption lines after March 22, however, the results may be of interest.

TABLE II

Nitrogen Exner and Haschek and Neovius	Intensity	*Nova* Bright Bands
3995	50	Band 3986–4008
4026	3	Band 4018–4050
4035	4	Center 4035
4042	5	
4097	3	Conflict with $H\delta$
4103	3	
4146	4	Center band 4146 (*He?*)
4176	3	Center band 4173 (*He?*)
4207	2	
4229	3	Band 4224–4246
4237	5	Center 4237
4242	5	
4348	2	Conflict with $H\gamma$
4426	2	Maximum 4425
4433	2	Band 4435–4450
4447	20	Center 4442
4508	2	
4515	1	Band 4508–4534
4530	2	
4601	5	Maximum 4600
4607	4	Center band 4605
4614	3	
4622	4	Center band 4622
4631	15	Center band 4632
4643	5	Center band 4641
4649	5	Center band 4649
5003	10	Band 4991–5032
5007	10	*He* 5016 and on later plate N_1 5007
5045	7	Conflict with *He* 5048
5497	6	
5535	6	
5667	9	Band 5667–5694
5680	12	Center 5681
5712	6	Red edge band 5711

In the region of spectrum considered by Giebeler there are 12 lines in the spark spectrum of radium for which he has found corresponding lines in the *Nova*. Of these we have been able to measure seven upon our photographs. Two of these, however, fall within the $H\gamma$ band and their agreement with radium lines is entitled to little significance on account of the presence of a great number of narrow dark lines, so many, in fact, that accidental coincidence would be almost certain. On two of the remaining five lines, λ 4153 and λ 4532, our measures show very close agreement with those of Giebeler and indicate discrepancies of over an Ångström unit from the radium lines.

In the region of wave-lengths longer than λ 4533 we find possible coincidences with λ 4600, λ 4642, λ 4693, and λ 4826. The first of these seems to be double in the *Nova* spectrum, and the discrepancy both for it and for λ 4826 is large. The extremely bright radium line λ 4683 does not appear to be represented in the *Nova*.

The degree of correspondence in the case of the emanation spectrum is about the same as for the radium spark, about 50 per cent of the lines having possible coincidences in the *Nova* spectrum. There are dark lines near the positions of the very intense lines λ 4167, λ 4350, λ 4609, and λ 4626, but none near λ 3982, λ 4203, and λ 4681. In general there seems to be very little agreement between the relative intensities of the emanation and the radium spark lines and the dark lines in the *Nova*, and the same fact seems to be true of Giebeler's results. Thus the four strongest radium lines (omitting λ 4341, which falls on the $H\gamma$ band) in the part of the spectrum investigated, λ 4178, λ 4305, λ 4436, and λ 4533, have been measured by him upon but one photograph, while several of the fainter lines have been measured more frequently.

In view of these results we do not consider the presence of the radium or the emanation spectrum in the *Nova* as established, at least for the period covered by our observations.

We have not been able to detect with any certainty evidence of a periodic variation in the structure of the bright hydrogen lines such as was suspected by Wolf,[1] but the dates of the observations

[1] *Astronomische Nachrichten*, **191**, 167, 1912.

PLATE XVI

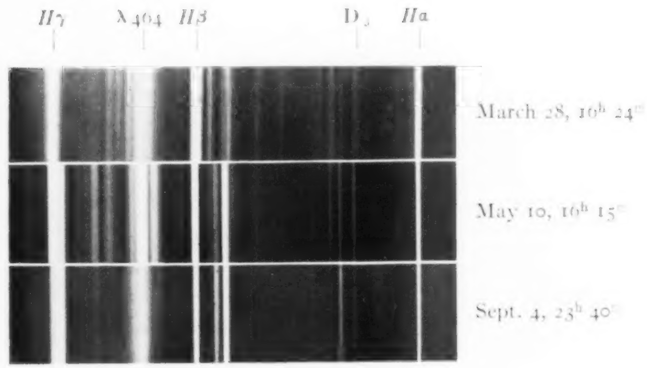

SPECTRA OF *Nova Geminorum* No. 2

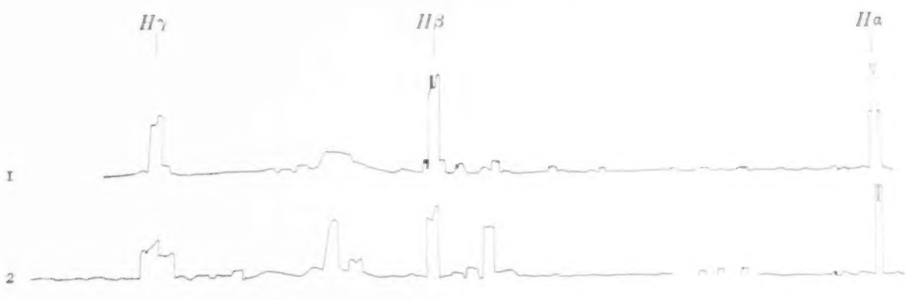

INTENSITY CURVES OF SPECTRA OF *Nova Geminorum* No. 2

1. March 28, $16^h\ 24^m$
2. May 10, $16^h\ 15^m$

PLATE XVII

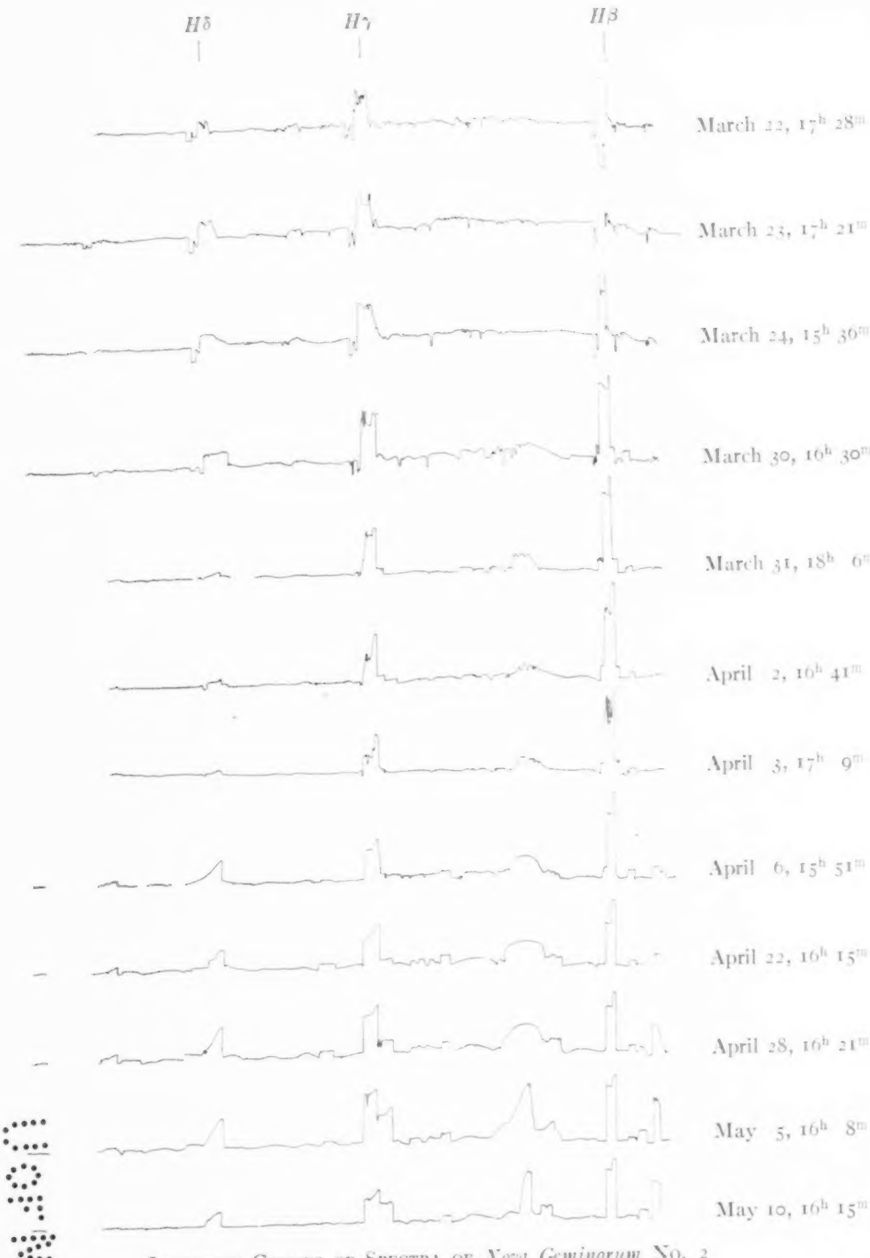

INTENSITY CURVES OF SPECTRA OF *Nova Geminorum* NO. 2

were not particularly favorable for such an investigation. It is perhaps worthy of note that there appears to be some evidence of a progressive change in the wave-lengths of the bright hydrogen bands during the period of rapid decrease in the light of the star, March 25–April 6. As the brightness grew less and the star more red in color the bands appeared to shift somewhat toward the red. It is possible that there may be a shift in the maximum of the individual bands with decrease of temperature similar to that found in a continuous spectrum.

The complex structure of the hydrogen bands led us to make an attempt to detect possible polarization in the spectrum of the star. Two spectrograms were obtained on April 7, using a Nicol prism and a quarter-wave plate in front of the slit. No displacement of the bright maxima was found when the quarter-wave plate was rotated. The dark hydrogen lines had become very faint at this stage of the development of the spectrum and are not visible on the photographs.

Since the above was written we have succeeded in obtaining two spectrograms of the *Nova* in the eastern sky. The first of these, γ 1472, was secured on August 19 and includes the portion of the spectrum between λ 4000 and λ 5000. The second, γ 1591, obtained on September 4, includes the entire spectrum from λ 4000 to $H\alpha$. On account of the low altitude of the star and the impossibility of giving a very long exposure because of the approach of daylight the second spectrogram was somewhat underexposed. Enlargements of the spectra are shown in Plates XV and XVI. The star appeared to be not far from the ninth magnitude at the time of these observations.

A comparison of these spectrograms with those obtained in the latter part of May indicates a further development of the spectrum of the star toward the nebular stage. The chief nebular line, λ 5007, is now considerably more intense than $H\beta$, and similarly the nebular line at λ 4365 is stronger than $H\gamma$. The second nebular line, λ 4959, and the line at λ 5757 have also increased greatly in intensity. On the other hand, the band at λ 4641 has become fainter and the principal series line of hydrogen at λ 4687 can hardly be distinguished at all. The helium lines

λ 4472 and λ 5876 are of about the same intensity as on the earlier photographs.

In the accompanying table are given the results of our measures of some of the more important bands and lines on these spectrograms, together with the results obtained from the photographs taken in the latter part of May.

	γ 1472 –γ 1591	Width Ångströms	γ 1185 –γ 1201	Width Ångströms
$H\epsilon$	3970.1	15.3	......	....
$H\delta$	4102.5	22.9	4102.6	24.9
Nebular	4269.6	19.2	4269.4	20.7
$H\gamma$ and nebular	4351.1	45.6	(4353.3)	(47.7)
	4442.5	15.8	4443.0	14.0
Helium	4473.3	20.3	4473.8	22.0
Nebular	4639.5	38.9	4640.8	....
$H\beta$	4862.6	25.7	4863.0	29.9
Nebular	4960.1	25.8	4960.1	27.8
Nebular	5007.9	28.5	5007.1	25.4
Nebular	5680.4	....	5680.2	27.2
Nebular	5757.4	26.3	5755.9	27.4
Helium	5878.2	....	5878.1	26.5
$H\alpha$	6566.5	35.8	6569.4	39.8

It is clear from this comparison that no very marked changes either in the wave-lengths or the widths of the bright bands have taken place in the interval of three months between the two series of observations. The widths of the bands are somewhat less on the later photographs, except in the case of one or two lines; but the difference is probably due in main to the fact that the density of the later negatives is less than that of the earlier series. In this respect, as has previously been stated, the bands resemble similar bright bands found in the spectra of Wolf-Rayet stars, and are widely different from the narrow sharp lines characteristic of the spectra of gaseous nebulae.

There appears to be a slight tendency toward a reversion to their normal wave-lengths of the centers of the bright bands, but the effect is too slight to be recognized with certainty. The marked change in the wave-length of $H\alpha$, and in a less degree of λ 5757, is due in all probability to the uncertainties of measurement in this part of the spectrum. A general displacement toward longer

wave-lengths of the centers of the bands is still a characteristic of the spectrum, as it was in the earlier observations.

An important feature of the bright bands is the persistence of the faint broad absorption bands crossing them, which have been observed throughout the entire series of photographs. They appear to be symmetrically placed on the bright bands and are present on the nebular bands as well as on those of hydrogen and helium. In some cases they seem to be broken up into narrow lines such as were found upon some of the earliest photographs. The nature of the absorption is such as is characteristic of a thin layer of absorbing gas of considerable density.

We are indebted to Miss Lasby and Miss Ensign for many of the measures upon the spectrograms, and to Miss Burwell for the intensity-curves drawn from the original negatives. The enlargements of the spectra are due to Mr. Ellerman.

Mount Wilson Solar Observatory
September 23, 1912

THE PRIMARY STANDARD OF LIGHT

By HERBERT E. IVES

A primary standard of light, properly to deserve the title, should be specified, as nearly as is possible, in terms of the fundamental units of length, mass, and time. No existing, so-called primary standards—the candle, the Hefner, the Violle, the pentane lamp—conform to this idea of a primary standard. In these latter the specification is in terms of physical and chemical quantities such as burner dimensions and fuel composition, which, while assuring the essential characteristic of *reproducibility*, can lay no claim to fundamental character.

The primary standard which should be defined is that of the quantity with which we are actually concerned in the use of light, namely, *luminous flux*, of which the present unit is the *lumen*. Luminous flux is flux of radiant energy of a certain quality, in virtue of which it is useful for illumination; the energy possessing, in short, the capacity to arouse through the eye the sensation of light or brightness. An immediate analysis resolves the specification of luminous flux into two parts, one physical, the other physiological. The physical part is rate of flow of radiant energy, directly expressible in fundamental physical units; the physiological part is the coefficient which evaluates or determines the efficiency of the radiant energy as a producer of the sensation of light.

The nearest approach, therefore, to a complete specification of light flux in fundamental units is attained in the specification of an energy flux, weighted according to its value as a producer of the sensation of light. Several suggestions for such a standard have been made. I proposed some time ago[1] *one watt of radiation of maximum luminous efficiency* as the unit of luminous flux, and suggested that it be determined by measuring both as radiation and as light a selected monochromatic radiation of

[1] "Energy Standards of Luminous Intensity," *Transactions Illuminating Engineering Society*, p. 258, April 1911; "Luminous Efficiency," *Electrical World*, June 15, 1911.

known luminous efficiency. The mercury green line (.546 μ) lying close to or at the maximum of visual sensibility appeared particularly suitable.[1] Strache[2] has proposed that the radiation from a source be resolved into a spectrum which shall fall upon a diaphragm cut to the shape of the luminosity-curve of the normal eye. After recombination the radiation is to be measured in absolute units and the values obtained from various sources will necessarily be proportional to their luminous intensities. Houstoun[3] along similar lines suggests the use of a special absorption screen, whose spectral transmission shall be as the visual luminosity-curve.

In order that any of these suggestions may bear fruit it is necessary to establish the relative efficiencies of various radiations, in other words, to determine the luminosity-curve of the average eye for a normal (equal-energy) spectrum. In order to determine this it is in turn necessary to possess a method of photometry which shall make possible the measurement of lights of different color.

Until recently the problem of heterochromatic photometry was far from solution. Consequently the establishment of a rational primary standard of light could not proceed beyond the stage of suggestion. (In passing it may be observed that the connection between the problem of heterochromatic photometry and the rational standard of light has not been widely noted.) Work which I have recently completed on the photometry of lights of different color makes it possible to put the proposal for a radiation primary standard of light flux in more definite form.

The complete discussion of the proposed radiation standard may best be divided into three parts: (1) the photometry of lights of different color; (2) the measurement of luminous efficiency; (3) specification of the radiation standard.

I. THE PHOTOMETRY OF LIGHTS OF DIFFERENT COLOR

The determination of the relative brightness of different colored lights has always been a difficult and unsatisfactory process. Various methods—visual acuity, persistence of vision, equality of

[1] Fabry and Buisson have lately made such a measurement. *Comptes Rendus*, **153**, 254.

[2] Abstract in *Proc. Amer. Gas Inst.*, **2**, 401, 1911.

[3] *Proc. Roy. Soc.*, A, **85**, 275, 1911.

brightness appearance, and lately the flicker method—all have been employed in the attempt to evaluate the different qualities of radiation on the basis of their common attribute of brightness, difficult as it is to separate the latter from the attribute of hue. Various physiological factors such as the Purkinje effect make the problem vastly complex, and until recently we had no definite information as to the relationship between the renderings of the different photometric methods, nor did we have sufficient information to justify adopting any one method as "right."

Recent work by the writer, now appearing in detail elsewhere,[1] has made possible a decision as to the best photometric method and conditions of measurement. It is found that the *flicker photometer* possesses the maximum number of attributes of a good system of brightness measurement where color differences exist. Its qualifications are as follows:

1. It possesses the greatest sensitiveness of any photometric method.

2. The results are more closely reproducible than those of other methods.

3. Things measured equal to the same thing measure equal to each other.

4. The sum of the measured values of the parts is equal to the measured value of the whole.

5. The results given by it agree, at high illuminations, with the estimates of equal brightness by the commonest photometric method (equality of brightness) when the disturbing subjective elements in the latter are eliminated either by the mean of many observations or by measurements performed with small hue differences.

The expression "the relative brightness of two colored areas" has no meaning unless the conditions of illumination and field-size are specified. Certain conditions must be taken as standard and values for other conditions derived therefrom. As a result of the work quoted the standard photometric conditions suggested are:

1. The flicker photometer should be used.

[1] "Studies in the Photometry of Lights of Different Color, I to V," *Phil. Mag.* (abstracts in *Physical Review*, 1911 and 1912).

2. An illumination of 25 meter candles on a magnesium oxide surface. (In accordance with the results of Section 3 below, this is to be expressed as a brightness given by $\frac{10^{-6}}{\text{luminous effic.}} \frac{\text{watts}}{\text{cm}^2}$ normal radiation per unit solid angle.)

3. A photometric field of 2° diameter, surrounded by a bright area of 25° diameter.

4. The measurements should be made by a normal eye.

In connection with condition 4 it is to be noted that different eyes vary in their color-sensitiveness. It is necessary, therefore, to determine the color-sensitiveness of a normal or average eye, and to use only such eyes in heterochromatic photometry, or correct the results of abnormal observers to the value holding for an average eye. I have recently determined for this purpose the luminosity-curve of a normal equal-energy spectrum for a sufficient number of eyes to justify calling the mean curve that of an average eye. The standard photometric conditions above outlined were used and eighteen observers of normal vision were measured. The resulting mean normal luminosity-curve is given below. The values are expressed in terms of the maximum = unity, and are as well a scale of luminous efficiencies of the spectral radiations in terms of the maximum.

TABLE I

LUMINOSITY-CURVE OF THE AVERAGE EYE UNDER STANDARD CONDITIONS FOR HETEROCHROMATIC PHOTOMETRY

(Relative Luminous Efficiencies of the Different Spectral Radiations)

λ	Relative Efficiency	λ	Relative Efficiency
.44μ	.029*	.57	.948
.45	.047*	.58	.875
.46	.073*	.59	.763
.47	.107*	.60	.635
.48	.154	.61	.509
.49	.235	.62	.387
.50	.363	.63	.272
.51	.596	.64	.175
.52	.794	.65	.104
.53	.912	.66	.068*
.54	.977	.67	.044*
.55	1.000	.68	.026*
.56	.990		

* Extrapolated.

It is to be noted that condition 4 may be fulfilled by correcting to normal the results of an observer whose luminosity-curve is known, or it may be closely approximated by taking the results of a large number of observers. Better still, there may be substituted for the eye some radiation meter arranged to weight the radiation in accordance with data such as that of Table I. Perhaps the photo-electric cell will serve. Table I is offered as giving the data to effect a working approximation to condition 4 above given in case either a method of correction or a substitute for the eye is used.

2. THE MEASUREMENT OF LUMINOUS EFFICIENCY[1]

The term "luminous efficiency" has long been used for an almost purely physical quantity—the ratio of a certain portion of the energy radiated from a source to the total radiated energy. True, this selected portion is radiation which can produce the sensation of light and is hence called "visible"; but from deep red to dark violet the brightness of the spectrum varies so enormously that any method of estimating efficiency that calls it all "light" of equal value is foredoomed to have scant connection with real luminous efficiency. On the other hand, the ratio used in photometry and engineering, namely, lumens per watt, is a true measure of luminous efficiency, although there is in the term no indication of the ideal maximum such as is suggested by expressing the efficiency value as a percentage.

Now all that is significant and desirable in the purely physical so-called "luminous efficiency" may be retained and brought into exact parallelism with the true efficiency expressed by lumens per watt. Let the radiations from a source be weighted according to their value as light-producers, in terms of the radiation of maximum light-producing power. The ratio of the sum of these weighted radiations to the whole radiation gives the efficiency of the radiation expressed as a percentage of what it would be were all the radiation of maximum light-producing power. To this ratio Drysdale has given the name "reduced luminous efficiency,"

[1] See Drysdale, "Luminous Efficiency," *Lond. Ill. Eng.*, p. 164, 1908; H. E. Ives, "Luminous Efficiency," *Trans. Ill. Eng. Soc.*, p. 113, 1910; P. G. Nutting, "The Luminous Equivalent of Radiation," *Bul. Bureau of Standards*, **5**, 261.

although it might better supersede the older "luminous efficiency" entirely and appropriate its name.

This efficiency is exactly parallel with lumens per watt. It is, in fact, the ratio of the lumens per watt of the radiation from the light-source compared to the maximum possible lumens per watt. Knowing the lumens per watt of a source, it is necessary to know only the maximum possible specific luminous output in order to determine its luminous efficiency, expressed in a percentage value of real significance.

The table which has been given for the brightness values of the normal spectrum for the average eye is at the same time a table of relative luminous efficiencies of the spectral colors. Expressed in terms of the maximum as unity, it is directly available for determining the ("reduced") luminous efficiency of a known energy distribution.

The value of luminous efficiency for any radiation may, then, in accordance with the subject-matter of this section, be obtained in either of the two ways:

1. The ratio of the total radiation weighted according to the luminosity-curve of the average eye (maximum value unity), to the total radiation.

2. The ratio of the specific luminous output of the radiation being measured (e.g., the lumens per watt) to the maximum possible specific luminous output (i.e., monochromatic radiation of wave-length approximately $0.550\ \mu$), or

$$\mu=\frac{K}{K_{\max}}$$

μ = luminous efficiency
K = specific luminous output of the radiation in question
$K_{\max}$ = maximum possible specific luminous output (that of the ideal source)

The *total* efficiency of a light-source is obtained, *upon the same scale*, by substituting "source" for "radiation" in (2), i.e., by taking the lumens per applied watt instead of radiated watt.

3. SPECIFICATION OF THE RADIATION STANDARD

Using the symbols and the definitions given above, we arrive at the following defining equations:

$$\text{Luminous flux} = KE$$

E = rate of flow of energy

K = specific luminous output of the radiation

$$= \mu K_{max} E$$

Now, E is expressed in C.G.S. units.

μ is a pure number determined by the physiological characteristics of the normal eye.

K_{max} is a quantity whose value is entirely dependent on the dimensions of the particular "primary" standard used in the system—Hefner, candle, or piece of hot platinum—and on the unit of energy flux.

The present proposal is:

1. *Make K_{max} = unity*
2. *Express E in watts*

whence *the unit of luminous flux is the flux from a source radiating energy of maximum luminous efficiency at the rate of one watt*, or, *it is the flux from a source of radiant luminous efficiency μ, radiating energy at the rate of $\frac{1}{\mu}$ watts.*[1] The quantity μ is of course to be determined by the general methods given above.

The absolute value of the unit of flux may in general be determined by measuring both in light and energy units a radiation of known luminous efficiency. As has been mentioned early in this paper, this may be done by several equivalent methods. For instance, a monochromatic radiation of known luminous efficiency may be measured in both ways. Or a "visual luminosity screen" may be used for the radiation measurement. The effect of the latter, when corrections are made for its minimum absorption, is to reduce all the radiation to the value it would have if of maximum luminous efficiency. This second method may be applied to known energy-distributions in the form of graphical calculation. Calculations of this sort made by applying the normal luminosity-curve to energy-distributions of known total value[2] indicate a value of K_{max} of about 800 lumens per watt.

[1] Or, the flux from a source of *total* luminous efficiency μ, *consuming* energy at the rate of $\frac{1}{\mu}$ watts.

[2] Ives, "Luminous Efficiency," *op. cit.*

Attention might be called to the fact that the problem of determining the so-called mechanical equivalent of light becomes identified with the establishment of the primary standard, since the latter is specified by the *least mechanical equivalent.*

The definitions of the other common photometric units follow directly from that of flux. For instance, the unit of intensity is the intensity in a certain direction of a source radiating in that direction unit flux per unit solid angle, that is, $\frac{1}{\mu}$ *watts per unit solid angle.*

Using the value $E_{max}=800$ lumens per watt and an albedo of 0.95 for $Mg\ O$, 25 meter candles becomes very nearly $\frac{10^{-6}}{\mu}\ \frac{\text{watts}}{\text{cm}^2}$ per unit solid angle, normal radiation; the value given under photometric condition 2.

SUMMARY

It is proposed that the unit of luminous flux be defined as the flux from a source radiating energy of maximum luminous efficiency at the rate of one watt. The method of estimating luminous efficiency, and the method of colored-light photometry which it is necessary to adopt preliminary to establishing the radiation standard, are described.

Physical Laboratory
National Electric Lamp Association
Cleveland, Ohio

THE INFLUENCE OF TEMPERATURE ON THE PHENOMENA OF PHOSPHORESCENCE IN THE ALKALINE EARTH SULPHIDES

By HERBERT E. IVES and M. LUCKIESH

In a previous paper[1] the present authors described experiments on the effect of infra-red radiation upon the phosphorescence of zinc sulphide. It was found that the effect of long-wave radiation is a function of the time which has elapsed since the termination of excitation. Shortly after excitation an exposure to red or infra-red causes a rapid drop in phosphorescent intensity, while later exposure causes a flash of light followed by a drop in brightness. The present investigation has grown out of attempts to obtain further information on this phenomenon by studying it under various changed conditions. Among these conditions temperature has proved so productive of results bearing not only upon the flashing-up phenomenon but upon other phases of phosphorescence as to warrant considering this paper as chiefly having to do with temperature and phosphorescent phenomena in general. The methods and procedure of the previous paper are closely followed, and reference should be made thereto for experimental details. The only essential difference in the apparatus consists in the uniform use of a quartz mercury arc and blue glasses in place of the carbon arc used before.

THE DECAY OF PHOSPHORESCENCE AT DIFFERENT TEMPERATURES

Various expressions have been proposed to represent the brightness of phosphorescence as a function of time since excitation. That most generally met is

$$I=\frac{1}{(a+bt)^2}\qquad \begin{array}{l} I=\text{brightness}\\ t=\text{time}\end{array}$$

which has a simple theoretical derivation, and has led to the common practice of plotting decay-curves in terms of $\frac{1}{\sqrt{I}}$ against time.

[1] "The Effect of Red and Infra-Red on the Phosphorescence of Zinc Sulphide," *Astrophysical Journal*, **34**, No. 3, 1911.

Becquerel found cases in which the empirical formula

$$I=\frac{1}{(a+bt)^n}$$

held for values of n other than 2.

In our previous work on zinc sulphide we found the latter expression with a value of $n=1.03$ ($I^{-0.97}=a+bt$), to accurately represent the decay-curve found.

Several observers have studied the effect of temperature on the rate of decay of phosphorescence. In general the rate of decay is greatly increased by rise in temperature. Micheli[1] gives data on several sulphides over a temperature range of several hundred degrees, but does not derive any expression connecting rate of decay with temperature. Pierce[2] in experiments on zinc sulphide and Balmain's paint finds a change of curvature of the $\frac{1}{\sqrt{I}}$ plots with change of temperature, and seeks for an explanation in the possible multiple character of the emission bands.

In the present work the samples of phosphorescent sulphide were placed on a shallow trough of nichrome strip, arranged to be heated electrically. A separate trough was arranged on a solid brass column around which melting ice could be packed for securing zero temperature. In some of the work the phosphorescent material was laid on the outside of a square brass tube into which carbon dioxide snow was rammed. The temperatures corresponding to various currents through the nichrome strip were determined by melting various low-melting metals. The values given are not to be taken as more than rough approximations, since the details of the apparatus were somewhat changed after the temperature calibration.

Several different sulphides were experimented with, but the majority of the experiments were made with the zinc sulphide previously used. Tests on other sulphides were largely for confirmatory purposes or were made incidental to other than purely temperature investigations. The sulphides besides zinc were Balmain's paint, *BaBiK* (from Leppin & Masche) and *SrZnFl* (our own preparation).

[1] *Arch. sc. phys. et nat.* (4), **12**, 5, 1901.

[2] *Phys. Rev.*, **26**, 314, 1908.

The results obtained have been very definite and clear cut. In every case we have found the decay-curves to be represented by the Becquerel equation

$$J^{-x}=a+bt$$

in which x is a function of the temperature, becoming smaller the higher the temperature.

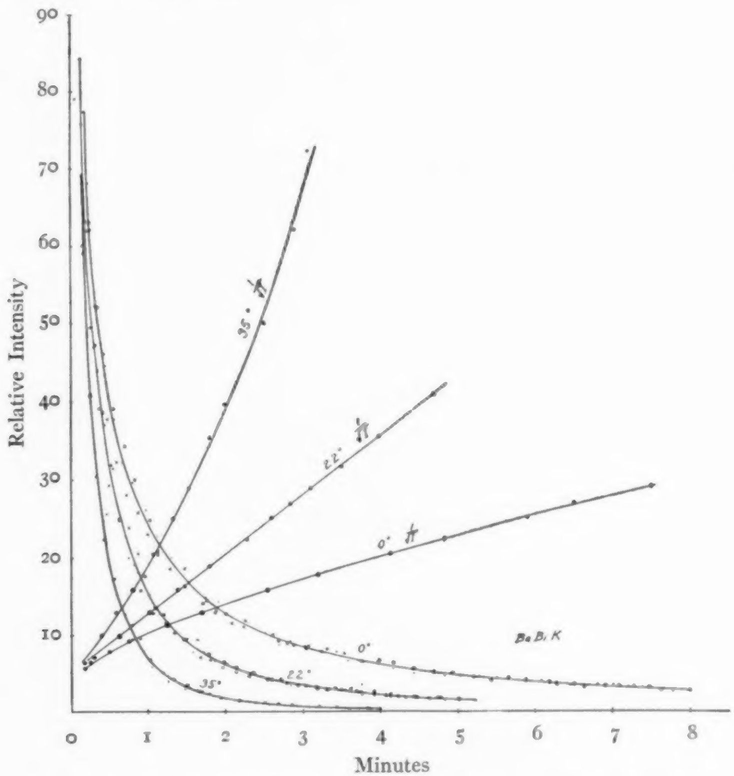

FIG. 1.—Decay of phosphorescence in *BaBiK* at different temperatures

Fig. 1 shows decay-curves at 0°, 22°, and 35° for the *BaBiK* sulphide, a compound which proved very sensitive to temperature change. When plotted in terms of $\frac{1}{\sqrt{I}}$ against time, the curve at 0° is concave to the time axis, that at room temperature is straight (taken alone this might easily have been interpreted as confirming

the value $\frac{1}{2}$ for x), while that at 35° is *convex* toward the time axis. Fig. 2 shows the straight lines which result on plotting the data with the value of $x=0.8$ for 0°, $x=0.5$ for 22°, $x=0.3$ for 35°. In Fig. 3 are given the straight lines obtained in a similar manner from our more extensive data on zinc sulphide, which, however, is less sensitive to changes of temperature. It will be noted that the value $x=0.5$ is in this case not at room temperature but at over 80° C.

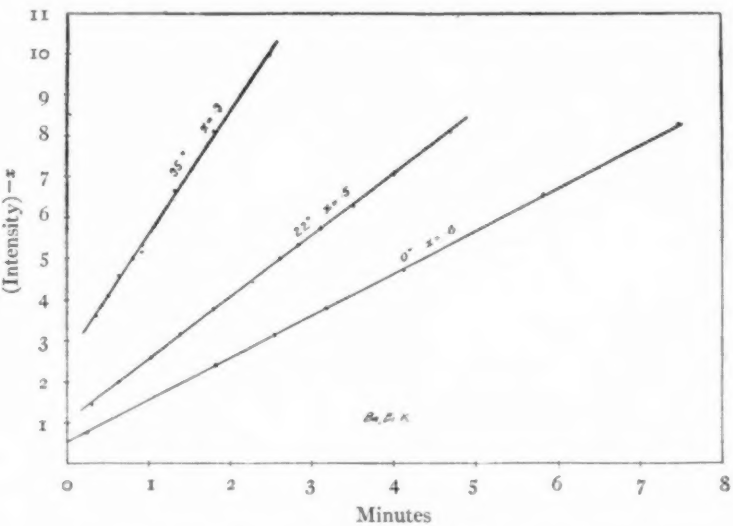

FIG. 2.—Decay of phosphorescence in *BaBiK* at various temperatures

The observation of decay-curves which plot convex to the time axis when drawn in terms of $\frac{1}{\sqrt{I}}$ (that is, with an exponent under 0.5) is not entirely new. Micheli's results for high temperature show this, Pierce found indications of such a curvature, and C. C. Trowbridge has obtained slightly convex curves in the case of gas phosphorescence. There has, however, been a tendency to look with suspicion upon such results, partly because they have been shown by data very near the limit of experimental accuracy, and doubtless partly because they are not compatible with the $\frac{1}{\sqrt{I}}$

formula. Curves concave to the time axis can be explained as summations of decays following the $\frac{1}{\sqrt{I}}$ formula, but *no summation of this sort will give a convex curve.* As the figures clearly show, our results are entirely unambiguous. We present the experimental formula, with the new significance of the exponent, as a function of temperature, merely for what it is worth as a means of represent-

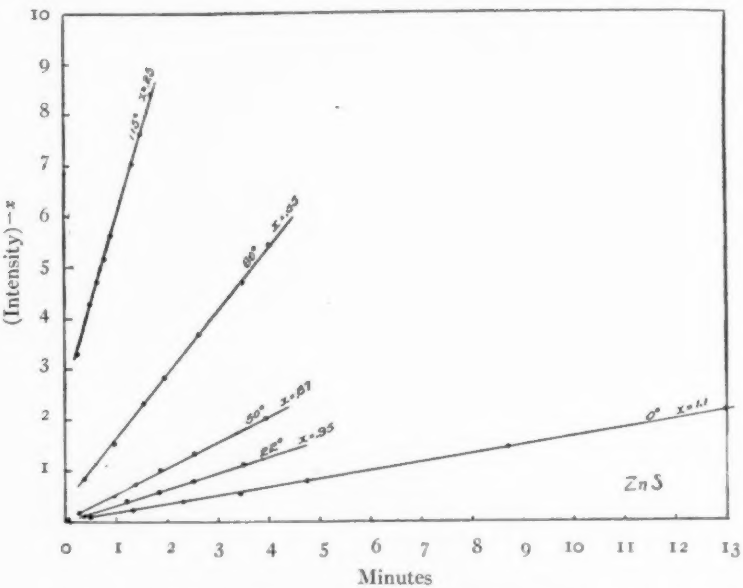

FIG. 3.—Decay of phosphorescence in zinc sulphide at different temperatures

ing the phenomena. It was tried in the first place without any guiding theory, and its only claim to notice is that it does represent, without exception, all the decay-curves we have obtained.

THE FLUORESCENCE AND INITIAL VALUE OF PHOSPHORESCENCE

From the formula $I^{-x}=a+bt$ the initial value of the phosphorescence may be calculated upon solving for the constants. We have done this for zinc sulphide, with the results shown in the dashed curve of Fig. 4. The full line shows observed values of the "fluorescence" made through a yellow glass which completely

absorbs the exciting blue mercury lines, and which has no effect on the measurements of phosphorescence. It is evident that the total fluorescence, and that part of it which persists as phosphorescence, are not one and the same thing. This idea is confirmed in other ways. The change from fluorescence to phosphorescence obeying the phosphorescence law takes place certainly within two or three seconds, for points on the decay-curve, obtained three seconds after excitation, fall exactly in their calculated place. As Lenard discovered, the light emitted during excitation is of two kinds, constituting what he calls the momentary and the permanent processes, the latter being predominant in the excitation caused by certain spectral regions. The momentary process is present prac-

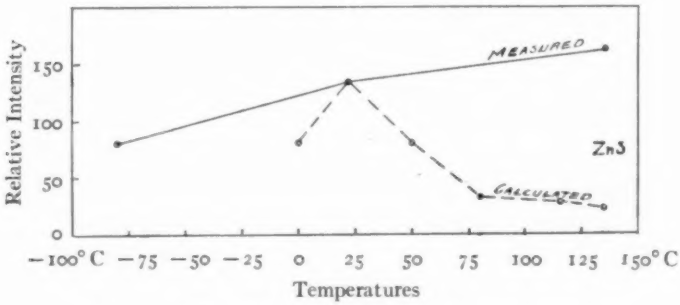

FIG. 4.—Relative initial intensities at various temperatures

tically only during excitation. By projecting a quartz mercury-arc spectrum on a zinc sulphide surface for a minute, and then obstructing the light, the two processes are clearly separated. The lines exciting the permanent process remain visible as phosphorescent strips, while strips which were equally bright during excitation but belong to the momentary process are almost instantly extinguished. The data of Fig. 4 are therefore capable of straightforward explanation in terms of other knowledge. It affords confirmation of Lenard's observation that at high and low temperatures the emitted light becomes more and more of the momentary variety. The excitation used throughout the work, as later study showed, consisted chiefly of three blue and near ultra-violet lines of the *Hg* arc located in the permanent process excitation region. The fluores-

cence intensity would have been relatively much higher than is shown in Fig. 3 had other "momentary" excitation regions been active.

VARIATIONS DUE TO COMPOSITION AND TREATMENT

Werner[1] has investigated the decay-curves of samples of the *SrZnFl* phosphor, in which the quantity of zinc was varied over a range of several thousand times. He found differences which he explained as due to various relative amounts of momentary and permanent process, the latter following the relationship $\frac{1}{\sqrt{I}}=a+bt$. His work was all done at room temperature. No "convex" curves were obtained. Had these been found they would have been difficult to reconcile with the suggested explanation.

In the expectation that these differences of composition might be equivalent to different temperatures and therefore capable of representation by different values of x in the above equation, we have made up a series of samples of this sulphide, following closely the procedure as given by Werner. Our samples ranged in relative composition from 1 to 100,000 parts of zinc, covering very nearly the same range in quantity as the ones used by Werner. These were measured for decay-curves at zero and at room temperature, with interesting results. By inspection it was found that all our samples had substantially the same brightness during excitation. But immediately upon extinction of the exciting light, the specimens of small zinc content decayed with great rapidity, the richer specimens displayed enduring phosphorescence, measurable for as much as five to ten minutes in the most favorable cases. The behavior of the different specimens appeared therefore to be parallel to that occasioned by different temperatures. The decay measurements, however, told a very different story. In every case where reliable measurements could be obtained an exponent of $x=1.0$ was found for zero temperature, of $x=0.8$ for room temperature. The difference in behavior of the samples of different quantitative composition appears to be represented merely by different values of the constants a and b of the equation here used. The exponent is a

[1] *Ann. der Physik*, **24**, 164, 1907.

characteristic of the phosphor and is varied by temperature alone.

The series of samples above described were all subjected to the same treatment in heating (in an electric furnace). Some experiments were made in variations of treatment. These resulted in brighter or duller phosphorescence but no certain effect on the value of the exponent was found.

INFRA-RED EFFECTS AND TEMPERATURE

The effect of infra-red on phosphorescence, which was the original problem before us, was studied at different temperatures, the experiments being confined to zinc sulphide. We were led to expect a dependence of the flash-up and extinction effects upon temperature by Lenard's observation that at very low temperatures zinc sulphide showed a strong, long-continued flash-up, in contrast to its fleeting or unnoticeable flash at room temperatures.

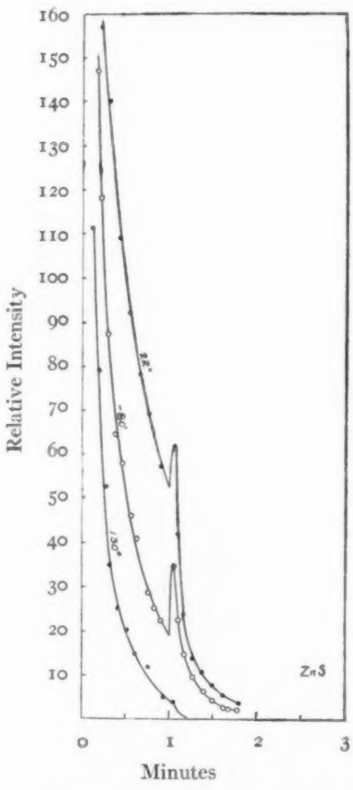

FIG. 5.—The flashing-up phenomenon under infra-red in zinc sulphide at different temperatures.

Fig. 5 gives a set of curves selected from a number which all show the same characteristics. At the temperature of melting carbon dioxide, $-80°$ C., the flash-up is very pronounced; at room temperature, $22°$ C., it is much less pronounced; at $130°$ C., entirely absent. It is therefore a low-temperature effect. In this connection it is to be remembered that different phosphors are in their permanent phase at different absolute temperatures, so that the same temperature may be high for one phosphor and low for another, each having in fact its own temperature scale. In this fact may lie

a partial explanation of the peculiar behavior of zinc sulphide. We find with other phosphors which show the flash-up—namely, Balmain's paint and *SrZnFl*—that the flash-up percentage increases in magnitude the greater the interval after excitation, and that it decreases in magnitude with any increase in temperature. With zinc sulphide at room temperature the behavior is very much as if the phosphor consisted of a mixture of components at very different effective temperatures. The "high"-temperature components which are immediately extinguished by infra-red at first predominate, leaving, later in decay, the low-temperature constituents to give the flash-up. In the other phosphors there is (on this hypothesis) immediately after excitation merely a somewhat larger proportion of the high-temperature components or the different components are only at slightly different effective temperatures, the flash-up percentage is less than it becomes later but is not masked by the effect of the high-temperature components. That these phosphors are very irregular in composition is a well-known fact, easily learned upon close inspection of the individual particles of a phosphorescent surface. Some particles are almost entirely of the momentary character; others are permanent. Differences in color are frequently visible. Of course this mixture hypothesis is far short of an explanation of the infra-red effect, but it suggests how the somewhat different behavior of the different sulphides may be differences merely of degree.

INFRA-RED EFFECTS AND COMPOSITION

The effect of different quantitative compositions on the flash-up effect in *SrZnFl* was studied, but no definite effects were found—a flash-up was always produced by infra-red, it increased with the time interval after excitation. We did not find the relationship suspected in the previous paper to which we were led by Werner's work and theory, namely that the flashing-up effect would be more marked in certain quantitative compositions than in others. We have, however, found that certain accidental differences of treatment which we were not able to control certainly do affect the magnitude of the flash. One sample, in fact, behaved almost like the *ZnS* in showing no flash at all in the early part of the decay.

INFRA-RED EFFECT DURING EXCITATION

It was noted by Nichols and Merritt that the effect of infra-red upon zinc sulphide is quite marked even during excitation, its effect being to decrease the brightness of the emitted light. According to Lenard's view the effect of infra-red is considered equivalent to a very great local increase of temperature in the phosphorescent centers. According to our results shown in Fig. 4 the effect of heat is in general to increase the brightness of the fluorescent light. According to Lenard's view, then, heat and infra-red together should give an even greater depression than infra-red alone. To test this point observations were made, through the yellow glass, as before, upon the emitted light during excitation, with and without infra-red, at room temperature and at $-80°$ C. Fig. 6 shows the results. It is at once evident that heat and infra-red act oppositely, since the intensity at $22°$ under infra-red is greater than the intensity at $-80°$ without infra-red. Had the phosphor when exposed to infra-red at $-80°$ been raised to $22°$ its brightness would have increased.

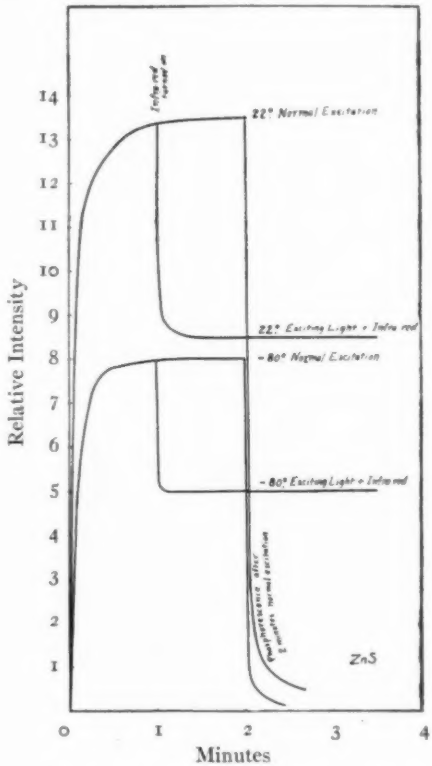

FIG. 6.—Effect of infra-red upon the intensity of the emitted light during excitation at $22°$ C and $-80°$ C.

EFFECT OF SIMULTANEOUS HEAT AND INFRA-RED UPON PHOSPHORESCENCE

Lenard's view that infra-red acts as a very high temperature localized in the phosphorescent centers was subjected to a test in

the case of phosphorescence, as well as in the case of fluorescence just described. The reasoning was as before. Experiment showed that a large increase of brightness or flash-up invariably occurred when the temperature of the decaying zinc sulphide was raised. There was no indication of an immediate extinction as in the case of infra-red action. In a recent paper Lenard[1] has shown that the

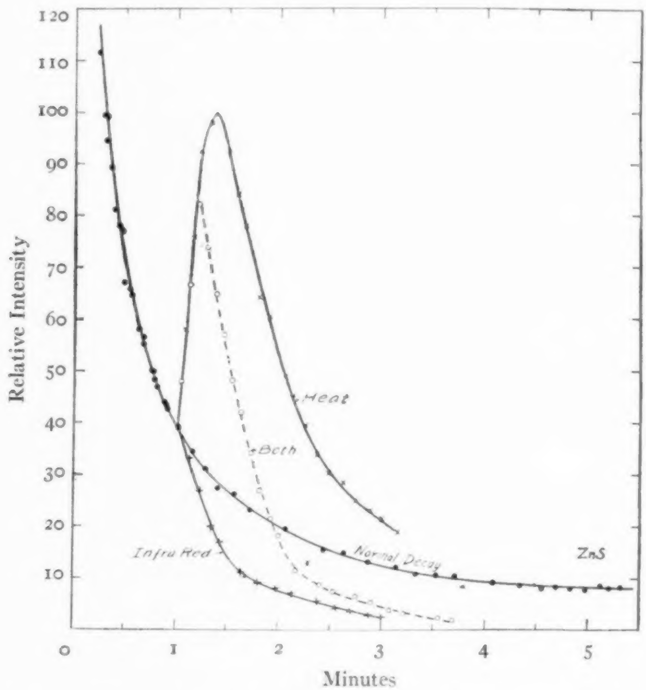

FIG. 7.—Effect of heat and infra-red upon the phosphorescence of zinc sulphide shortly after excitation.

total light given out by a phosphor is the same whether it decays naturally or is stimulated by heat; but that this is not true when infra-red acts. This peculiarity he ascribed to a radical disturbance of the light storing and emitting mechanism due to the intense heating by infra-red. If the effect of infra-red is really identical to

[1] "Lichtsummen bei Phosphore," *Sitzung. der Heidelberger Akademie der Wissenschaft*, **5**, 1912.

a greatly increased temperature localized in the emission center, it would seem reasonable to suppose that the two heating effects would add if applied simultaneously. Since the increase in temperature necessary to cause a flash-up is a small fraction of that ascribed to the local action of infra-red the effect of gently heating the whole phosphor may be expected if anything merely to increase the effect of infra-red; that is, if the two are applied shortly after excitation, to cause a greater drop in brightness in our zinc sulphide than infra-red would alone.

The apparatus was so arranged that either infra-red or heat could be applied to the phosphor, or both together. Fig. 7 shows the normal decay-curve, the flash given by gentle heating, the extinction caused by infra-red, and finally the effect of heating and infra-red exposure together. Instead of the heat supplementing the infra-red it is found that they oppose each other, the result being the summation of the separate effects. This appears to us to call for a modification of Lenard's idea of the infra-red effect.

EFFECT OF INFRA-RED ON THE DIFFERENT SPECTRAL EXCITATION REGIONS

By projecting a mercury arc spectrum by a quartz prism train upon our zinc sulphide it has been possible to determine to which excitation process the extinction and flashing effects belong. Taking advantage of the fact that with this phosphor the effect of infra-red is visible even in the emission during excitation, an infra-red image of a Nernst glower was projected lengthwise through the mercury spectrum. The result was definite information that infra-red affects only the permanent process, or phosphorescence. The dark valley cut through the mercury line images scarcely touched the lines which belong to the momentary process, i.e., those that are extinguished almost instantly by the removal of the exciting light.

This experiment disposes of a hypothesis put forward in our previous paper, namely, that the early extinction effect of the infra-red is to be ascribed to a large proportion of momentary process in this part of the decay, the momentary process being assumed to be extinguished at once by infra-red. All the peculiarities noted

as due to long-wave radiation are apparently to be ascribed to the permanent process.

SUMMARY AND DISCUSSION

The matter presented in this paper is almost wholly experimental. Where it has touched upon current theories of phosphorescence, as in the case of the relation between heat action and infra-red action, it has been destructive rather than constructive. The experimental results may be summarized as follows:

1. The decay of phosphorescence in the alkaline earth sulphides is accurately represented by the formula

$$I^{-x}=a+bt$$

where x is a function of the temperature, independent of the quantitative composition of the phosphor, and where a and b are functions of the composition and heat treatment of the sulphide.

2. The flashing-up phenomenon, under infra-red, is greatest at low temperatures, and decreases at high temperatures. It always shows an increase in magnitude with lapse of time after excitation.

3. In the case of zinc sulphide, infra-red and heat act, during excitation, and during the early part of decay, oppositely.

4. The effect of infra-red is upon the permanent process alone.

The suggestion made above, that these phenomena may be partially linked together by taking into account the complex character of the phosphors, is as far as we care to venture in the way of hypothesis at present. It is significant that decay-curves of the type obtained may be built up of terms of the form

$$i=ae^{-kt}$$

the law of mass action with one substance changing. Variations of a and k with temperature could produce the observed changes in the decay. Ascribing to each component its own temperature scale, the ordinarily prepared phosphor would consist of a mixture of different effective temperatures. The early part of the decay would be given chiefly by the high-temperature components, the later part by the low. Simply noting that the flash-up effect is a low-temperature

effect enables us to picture why it becomes more marked as decay proceeds, without, however, giving any insight into the actual process which is thus different at high and low temperatures. The fact that the infra-red effect is localized in the spectrum, usually in two bands, would suggest, in view of the connection recently shown between phosphorescence and the selective photo-electric effect in the violet, that a study of the photo-electric effect in this zinc sulphide when exposed to infra-red both during excitation and during decay would be of interest.

Physical Laboratory
National Electric Lamp Association
Cleveland, Ohio

NOTICE

The scope of the ASTROPHYSICAL JOURNAL includes all investigations of radiant energy, whether conducted in the observatory or in the laboratory. The subjects to which special attention is given are photographic and visual observations of the heavenly bodies (other than those pertaining to "astronomy of position"); spectroscopic, photometric, bolometric, and radiometric work of all kinds; descriptions of instruments and apparatus used in such investigations; and theoretical papers bearing on any of these subjects.

Articles written in any language may be accepted for publication, but unless a wish to the contrary is expressed by the author, they usually will be translated into English. Tables of wave-lengths will be printed with the short wave-lengths at the top, and maps of spectra with the red end on the right unless the author requests that the reverse procedure be followed.

Accuracy in the proof is gained by having manuscripts typewritten, provided the author carefully examines the sheets and eliminates any errors introduced by the stenographer. It is suggested that the author should retain a carbon or tissue copy of the manuscript, as it is generally necessary to keep the original manuscript at the editorial office until the article is printed.

All drawings should be carefully made with India ink on stiff paper, usually each on a separate sheet, on about double the scale of the engraving desired. Lettering of diagrams will be done in type around the margins of the cut where feasible. Otherwise printed letters should be put in lightly with pencil, to be later impressed with type at the editorial office, or should be pasted on the drawing where required.

Where an unusual number of illustrations may be required for an article, special arrangements are made whereby the expense is shared by the author or by the institution he represents.

Authors will please carefully follow the style of this JOURNAL in regard to footnotes and references to journals and society publications.

Authors are particularly requested to employ uniformly the metric units of length and mass; the English equivalents may be added if desired.

If a request is sent *with the manuscript*, one hundred reprint copies of each paper, bound in covers, will be furnished free of charge to the author. Additional copies may be obtained at cost price. No reprints can be sent unless a request for them is received before the JOURNAL goes to press.

The editors do not hold themselves responsible for opinions expressed by contributors.

The ASTROPHYSICAL JOURNAL is published during each month except February and August. The annual subscription price is $5.00; postage on foreign subscriptions, 62 cents additional. Business communications should be addressed to *The University of Chicago Press, Chicago, Ill.*

All papers for publication and correspondence relating to contributions should be addressed to *Editors of the* ASTROPHYSICAL JOURNAL, *The Uuiversity of Chicago, Chicago, Illinois, U.S.A.*